

# Architected Hydrogels for Functional Tissue Engineering Applications

*Doris Zauchner, Monica Zippora Müller, Sophie Zengerle, Adam Aleksander Korczak, Muriel Alexandra Holzreuter and Xiao-Hua Qin\**

ETH Zurich, Institute for Biomechanics  
Leopold-Ruzicka-Weg 4, 8093 Zurich, Switzerland

\*E-mail: [qinx@ethz.ch](mailto:qinx@ethz.ch) (Corresponding author)

Tel: +41 (0) 44 633 78 44

## Abstract

The functionality of many biological tissues relies on their highly sophisticated architecture. Recent advances have enabled *in vitro* generation of human organoid models through 3D stem cell culture in animal-derived protein hydrogels. However, these oversimplified materials often lack *in vivo*-like microarchitecture and mechanical stimuli to support *in vitro* tissue formation. As such, there is an imperative need to develop architected hydrogels that can be integrated with 3D cell culture and microfluidic technologies to provide native-like dynamic 3D environments promoting multicellular self-organization and tissue maturation. In this review article, we provide an overview of the design and properties of architected hydrogels and highlight their integration with other bioengineering tools for functional tissue engineering. Firstly, we discuss the structural and physical properties in natural nanofibrillar hydrogels and synthetic analogues with non-linear elasticity. We then provide a comparative summary of different methods to generate macroporous hydrogels that facilitate mass transport, cell-cell communication, and tissue maturation in 3D. Next, we investigate examples of 3D printed hydrogels with complex tissue-mimicking architectures and discuss emerging applications of architected hydrogels in tissue engineering, organ-on-chip technology and mechanobiology. Lastly, existing challenges and future directions in developing architected hydrogels towards functional tissue engineering are highlighted.

## 1. Introduction

Most human tissues consist of sophisticated architectures across several length scales. For instance, human cortical bone is an architected material consisting of thousands of structural units – the osteons (**Figure 1A**).<sup>1</sup> Within each osteon, bone vasculature travels through the Haversian canal that has a porosity in the range of 20 - 40  $\mu\text{m}$ . Additionally, the canaliculi are nanoscale channels that enable embedded osteocytes to interconnect and sense fluid flow to regulate bone formation and resorption.<sup>2</sup> Similarly, skeletal muscle<sup>3</sup>, tendon<sup>4</sup>, and ligament<sup>5</sup> are complex tissues consisting of hierarchically structured fibrils that are essential for their adaptation to mechanical loads.<sup>6</sup> The adaptation of human muscle to mechanical stimuli is a complex process spanning eight orders of magnitude in length (Figure 1B). Engineering living tissues<sup>7</sup> that closely resemble these *in vivo* counterparts is not only a consideration of material choice, biocompatibility and matrix mechanics. In fact, tissue architecture has received increasing attention in the design of *in vitro* systems since biophysical cues<sup>8</sup> can strongly affect cell fates (differentiation, proliferation), 3D self-organization and *in vitro* tissue formation.

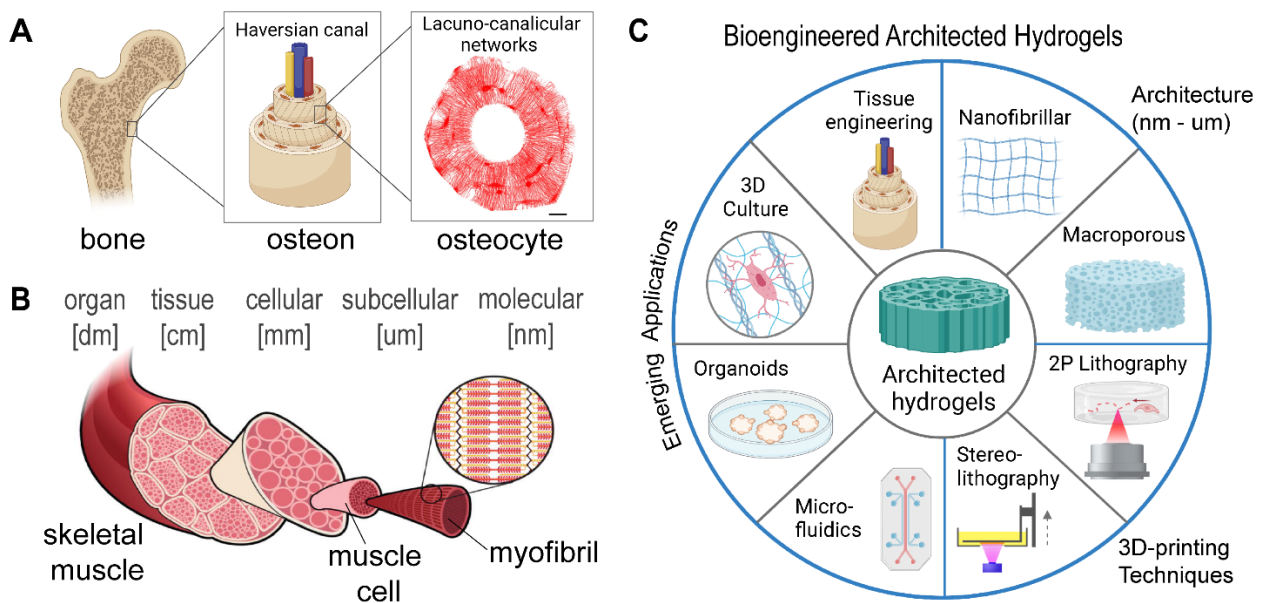


**Figure 1.** (A) Human cortical bone consists of many structural units named “osteons” in which the vasculature travels through the Haversian canals (20 - 40 microns), whereas osteocytes are deeply buried in the lacuno-canalicular networks (ca. 310 nm in diameter) that are crucial for bone mechanotransduction. Created in BioRender.com. The confocal image is adapted from Ref.<sup>9</sup>, licensed under a Creative Commons Attribution License. Scale bar = 50  $\mu\text{m}$ . (B) Human muscle adapts to mechanical stimuli from the molecular to the organ scale. Aligned myofibrils make up the muscle cell or muscle fiber. Adapted from Ref.<sup>3</sup> with permission of Springer Nature. (C) Hydrogels with a nanofibrillar or macroporous architecture have shown great promise for emerging applications in 3D cell culture, microfluidics and functional tissue engineering.

Despite immense efforts, recreating native-like tissue architectures *in vitro* remains a major challenge. Recent years have witnessed the use of hydrogels to cultivate cells in a 3D environment. However, synthetic

hydrogels lacking a fibrillar or microporous architecture show restricted cell viability due to the diffusion limit for nutrients and oxygen and inadequate mechanical cues. As such, it is important to consider porosity and biomechanical stimuli as essential aspects of the tissue engineering process. As the relevance of these properties has become evident for engineered tissue constructs in recent years, many researchers have attempted to use this knowledge to develop novel architected biomaterials, especially hydrogels, and to optimize their fabrication processes for functional tissue engineering applications. This allows for the fabrication of well-defined 3D environments that provide the basis for the application of further stimuli such as interstitial fluid flow. With the advance of these novel techniques, 3D engineered tissue constructs of bone and muscle,<sup>10-12</sup> vascularized organoids<sup>13</sup> or organ-on-chip systems<sup>14</sup> with 3D architecture and controlled mechanical environments are realizable and will most likely become valuable tools, not only for fundamental research but also for translational science and clinical applications in the future.

In this review, we seek to summarize recent developments in architected hydrogels for functional tissue engineering applications (Figure 1C). Firstly, we provide an overview of fibrillar hydrogels of natural and synthetic origin as well as their structure-function relationships. Since porosity plays a crucial role for 3D cell growth and tissue maturation, we then provide a comparative summary of a variety of methods to generate macroporous hydrogels to facilitate mass transport, cell-cell communication, and network formation. Next, new techniques to sculpture architected hydrogels by means of light-assisted 3D printing are reviewed since well-established techniques such as electrospinning and extrusion-based bioprinting are limited by their resolution, and hierarchical architectures in many different tissues require nano- to micrometer scale features. We then present how such architected hydrogels have been used for emerging applications in tissue engineering, for instance, in combination with microfluidics to engineer organ-on-chip *in vitro* systems and how these devices have been utilized for mechanobiological studies. Lastly, we discuss challenges that remain with these novel research tools and provide an outlook summarizing future directions towards functional tissue engineering.

## 2. Fibrillar Hydrogels

Cells and their native environments are fascinating composites of biopolymers synergistically acting to enable many important functions such as cell division and motility. A common feature of the extracellular matrix (ECM) and the intracellular cytoskeleton are fibrillar structures (**Figure 2**). As those biopolymer networks are embedded in water, they can be considered hydrogels. It is appreciated that the physical properties of ECM are strongly related to its inherent filamentous architecture. Fibrillar hydrogels are thus promising scaffolds for tissue engineering, 3D cell culture and regenerative medicine. The following subsections will give an overview of natural and synthetic fibrillar hydrogels and discuss their structure-function relationship such as the strain-stiffening effect.

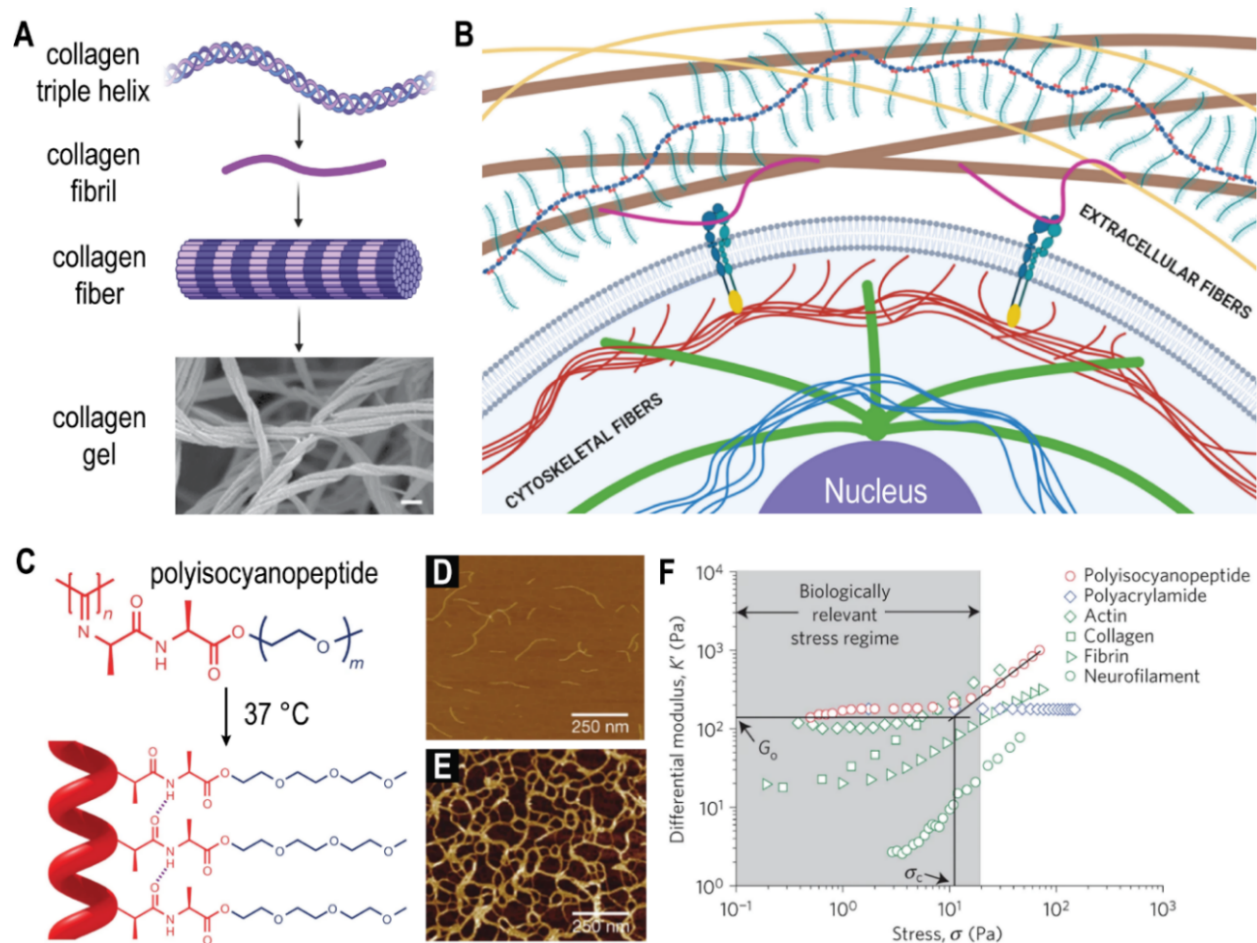


**Figure 2.** (A) Schematic of the assembly of collagen triple helix into fibrils, collagen fibers and a collagen gel. Scale bar = 200 nm. (B) Schematic representation of the fibrillar structures supporting the cells in tissues. Cytoskeletal fibers are depicted in red (actin), blue (intermediate filaments) and green (microtubuli). Cells adhere to the extracellular matrix (ECM) by attaching to binding sites on macromolecules such as fibronectin using integrins. The ECM consists of several components, for example collagen (brown), elastin (yellow) or proteoglycans (blue-red-turquoise). (C) Assembly of synthetic polyisocyanopeptide (PIC) hydrogels. AFM image of isolated PIC chains (D) and bundled PIC fibers after gelation (E). (C), (D) and (E) adapted from Ref.<sup>15</sup> with permission of Springer Nature. (F) Biopolymer gels exhibit stress-stiffening when exceeding a critical stress  $\sigma_c$ . Differential modulus,  $K'$ , as a function of stress,  $\sigma$ .  $G_0$  denotes the equilibrium bulk stiffness. Adapted from Ref.<sup>16</sup> with permission of Springer Nature.

## 2.1 Natural Fibrillar Hydrogels

Fibrous networks in the natural ECM consist of a variety of different macromolecules. Depending on tissue type and location they vary in composition. For example, the ECM of cartilage tissue is composed of type II collagen and elastic fibers.<sup>17</sup> Other tissues such as the dermis include high amounts of aligned collagen fibers which are essential to withstand high tensile loads.<sup>18</sup> Natural fibrillar hydrogels have been widely used in 3D cell culture and tissue engineering. For example, ECM-mimetic collagen and fibrin gels are the gold-standard materials for generating *in vitro* models of bone,<sup>19</sup> skin,<sup>20</sup> tendon and ligament.<sup>21</sup>

## Collagen

Type I collagen hydrogel has been frequently used as a 3D fibrillar matrix for cell culture given its proteolytic degradability, large mesh size and permissiveness for cell growth. The architecture of natural fibrillar gels is crucial for their performance. The fibril diameter in collagen is in the range of 70-150 nm, whereas the gel stiffness can be tuned from 10 Pa to 600 Pa depending on the protein concentration (**Table 1**). While their bulk mechanical stiffness is crucial to consider for a specific application, increasing attention has been drawn to the role of fiber architecture in determining cell fate. Fiber alignment has been shown to induce structural anisotropy, which strongly affects cell function, differentiation, and the direction of cell migration. For instance, recent studies in cancer biology demonstrated that collagen fiber structure can guide 3D motility of cytotoxic T lymphocytes or sarcoma cells.<sup>22-23</sup> Pruitt et al. showed that human cluster of differentiation 8 positive (CD8+) T cells migrated faster and more persistently in aligned collagen fibers than nonaligned ones.<sup>23</sup> Riching et al. found that matrix topography, rather than stiffness, is the dominant feature by which an aligned 3D collagen matrix enhances tumor cell invasion.<sup>24</sup> Collagen architecture and the structural organization of the fibers was also studied to determine the functional relationship across different tissues like the pulmonary heart valve cusp or the posterior pole of the eye.<sup>25-26</sup>

**Table 1:** Structural and physical properties of nanofibrillar hydrogels of natural and synthetic origins.

Hydrogel type	Fiber or fibril diameter (nm)	Permeability (cm <sup>2</sup> )	Stiffness (Pa)	Mesh Size (μm)	Notes	Refs
Collagen	70-150	1x10 <sup>-8</sup>	10-600 <sup>a</sup>	5-12	Properties are dependent on collagen concentration and gelation temperature.	27-29
Fibrin	40-150	0.11x10 <sup>-9</sup> - 7.5x10 <sup>-9</sup>	90-1,050 <sup>a</sup>	1-10	Measurements are based on fibrin gels from either animal fibrinogen or human plasma.	30-32
PIC	2-8	–	100-1000 <sup>a</sup>	0.03- 0.15 <sup>b</sup>	Properties are dependent on polymer concentration and gelation temperature.	15-16, 33

Polyisocyanopeptide (PIC). <sup>a</sup> Shear storage modulus. <sup>b</sup> Determined by small angle X-ray scattering (SAXS).

## Fibrin

As the fibrous material in blood clotting, fibrin gels have been widely used in 3D cell culture and tissue engineering. Fibrin gels are composed of self-assembled fibrils with a diameter in the range of 40 - 50 nm. Depending on the concentration of precursors (fibrinogen, thrombin, FXIII) and ionic strength, the stiffness of fibrin gels can be tuned in a wide range from 100 Pa to 1 kPa. Sasaki et al.<sup>34</sup> demonstrated that cells aligned parallel to the strain direction in a fibrin gel due to the structural changes of fibrin fibers. The resulting cellular patterning resembled that of tendon tissue. In addition to the structural properties of natural

fibrillar gels, the strain-stiffening effect may influence the behavior of cells in the gels. Winer et al.<sup>35</sup> showed that spreading of fibroblasts on soft fibrin hydrogels resembles the behavior observed on a much stiffer polyacrylamide gels. They hypothesized that this deviation is caused by the strain-stiffening behavior of fibrin. In addition, deformation of the matrix by the cells and the resulting stiffening of the gel increased cell elongation and alignment. Despite numerous advantages, natural fibrillar hydrogels also have obvious drawbacks, such as batch-to-batch variation, quick degradation, limited availability, and control over architectural and mechanical properties as well as their high price. Thus, the development of synthetic fibrillar hydrogels is highly desirable.

## **2.2 Synthetic Fibrillar Hydrogels**

Most conventional synthetic hydrogels are covalently crosslinked polymer networks composed of flexible monomers ( $L_p \ll L$ ). The mesh size in these networks is typically in the range of 5 – 80 nm, which often limits cell outgrowth, migration, and 3D multicellular self-organization. Synthetic fibrillar hydrogels, however, similar to natural fibers, have a greater  $L_p$ , offering equivalent stiffness at much lower volume and larger mesh size resulting in more permissive matrices. Recently, researchers have attempted to replicate the formation of semi-flexible fibers and the strain-stiffening behavior in synthetic biomaterials. A prominent example of this class of materials are polyisocyanopeptide-based hydrogels (PIC gels) developed by Kouwer et al. (Figure 2C).<sup>36</sup> They offer the unique ability to decouple the strain-stiffening behavior from the architecture, stiffness, and ligand density. This can be used to study the mechanical properties of cellular microenvironments separately. For example, Arg-Gly-Asp (RGD) peptide-modified PIC gels have been shown to direct stem cell commitment depending only on the onset of strain-stiffening.<sup>16</sup> Despite the many advantages of PIC systems, the polymer comes along with important drawbacks such as poor degradability and limited permissiveness. Apart from PIC, synthetic fibrillar hydrogels were also obtained through the self-assembly of synthetic molecular gelators forming semi-flexible fibers.<sup>37</sup> Strain-stiffening synthetic hydrogels were also reported to form via self-assembly of bolaamphiphiles which result in semi-flexible chains.<sup>38</sup>

## **2.3 Synthetic Electrospun Fibrous Hydrogels**

A different approach to create fibrillar hydrogels, even though often referred to as a 2.5-dimensional scaffold, is electrospinning. Nanofibers produced with this method are typically stiffer and greater in size than self-assembled semi-flexible chains. In contrast to semi-flexible chains, they do not show strain-stiffening behavior in the cell-accessible regime in most cases. Their advantage is the high porosity which can be used by cells to migrate and the high diffusivity of biochemical signals such as growth factors and nutrients. A seminal work by Burdick and co-workers used complementary chemical moieties in electrospun fibers which were shown to self-adhere, plastically deform, and stiffen upon mechanical strain (**Figure 3**) thus

recreating the strain-stiffening property of native fibrillar hydrogels. Other pioneering work has been accomplished by producing protease-sensitive electrospun fibrous hydrogels by Burdick and co-workers.<sup>39</sup> The authors demonstrated that these hydrogel matrices are susceptible to protease-induced degradation *in vitro* in a protease dose-dependent manner and *in vivo* in a subcutaneous mouse model. Significant advancements in the electrospinning design across numerous tissue engineering applications have been achieved and described in latest reviews.<sup>40-42</sup>

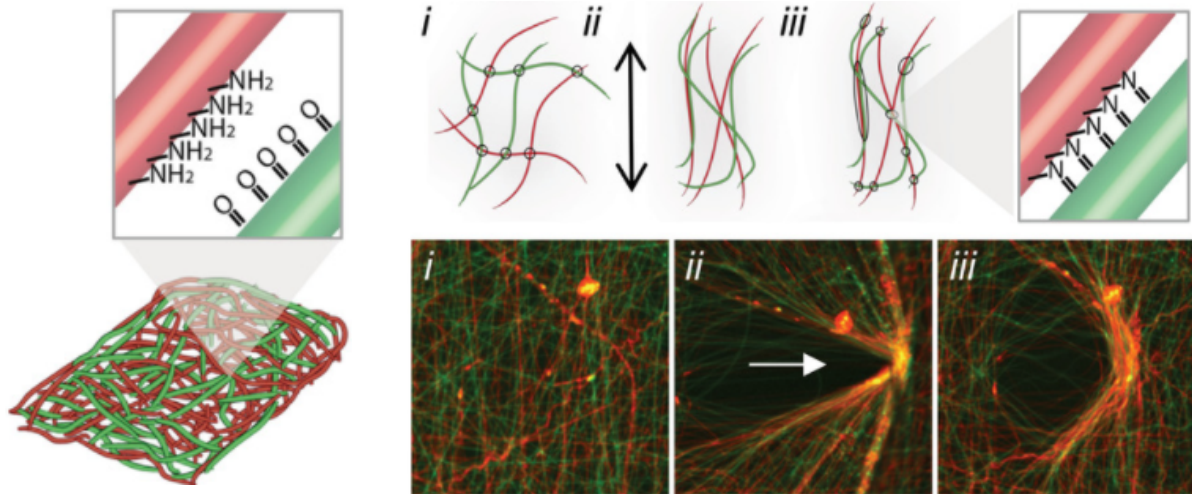


**Figure 3.** Electrospun hyaluronic acid fibers modified with complementary chemical moieties i.e., hydrazides (red) and aldehydes (green) were shown to self-adhere, plastically deform, and stiffen upon mechanical strain. i) before, ii) during, and iii) after applying strain. Adapted from Ref<sup>43</sup> with permission from WILEY.

## 2.4 Structural and Physical Properties of Fibrillar Hydrogels

Fibrillar hydrogels exhibit structural and physical properties distinct from molecular hydrogels due to their unique structure. These properties may impact cell survival and cell fate. Thus, a deeper understanding of the impact of the fibrillar structure on physical properties as well as the ability to tailor these properties is highly desirable.

### *Structural properties*

During the formation of fibrillar hydrogels, individual building blocks firstly associate into fibrils or fibers through hydrogen bonding, hydrophobic interactions, ionic interactions and  $\pi$ - $\pi$  stacking. The formed fibrils or fibers then assemble into a network by entanglement, branching or association. Depending on the initial building blocks, the aforementioned interactions contribute to the network formation to different extents which in turn influences the properties of the resulting fibrillar hydrogel.<sup>44</sup> For example, Nagy-Smith et al.<sup>45</sup> found that fibrillar hydrogels formed from a racemic mixture of MAX1 and DMAX1 displayed increased

stiffness compared to hydrogels of either one of the peptides due to a higher number of hydrophobic interactions in the core of the fibrils.

The mesh size of fibrillar hydrogels depends on the initial concentration of building blocks as well as the density of crosslink points.<sup>46</sup> Overall, pore size tends to be larger for fibrillar than for molecular hydrogels<sup>44, 47</sup> thus improving mass transport inside the hydrogels because diffusion of molecules smaller than the mesh size is only minimally affected by steric hinderance.<sup>46</sup> Further, fiber alignment reduces the flow resistance parallel to the fibers.<sup>48</sup> Increased transport of nutrients and waste inside fibrillar hydrogels support cell survival and growth, and larger pore sizes allow for cell migration.<sup>49</sup>

In fibrillar hydrogels, clusters of cell adhesion ligands are present on the surface of the fibers similar to *in vivo* conditions.<sup>44</sup> Such clusters of RGD peptides have been shown to increase fibroblast spreading and speed compared to unclustered RGD.<sup>50</sup> The incorporation of ligands is facilitated by the modular nature of fibrillar hydrogels allowing the functionalization of individual building blocks prior to their assembly into hydrogels.<sup>50-52</sup> Following the same approach, growth factors and signaling molecules can be incorporated into fibrillar hydrogels.<sup>50, 52</sup>

### *Mechanical properties*

The elastic properties of hydrogels can generally be described by the storage modulus ( $G'$ ) of the material, which is influenced by the stiffness of individual fibers as well as the network mesh size in fibrillar hydrogels.<sup>45, 53</sup> Stiffer fibers and denser, more-crosslinked networks increase  $G'$ .<sup>45</sup> In synthetic fibrillar hydrogels, mesh size can be controlled through the polymer concentration of the hydrogel<sup>53-54</sup>, whereas fiber stiffness can be modulated by changing the physical interaction strength between fibrils<sup>53</sup> or by the introduction of chemical crosslinks.<sup>55</sup> Taufalele et al.<sup>56</sup> found that at lower polymerization temperatures, the fiber diameter in collagen matrices increases and that this increase in diameter leads to enhanced stiffness of the fibers at the microscale. In addition, they found that the compliance of aligned collagen matrices is higher at the microscale than for random matrices, possibly due to a reduction in the interconnectivity of fibers.

### *Strain-stiffening Effect*

Biopolymers, depending on the persistence length ( $L_p$ ) and the contour length ( $L$ ), can be categorized into flexible ( $L_p \ll L$ ), semi-flexible ( $L_p = L$ ) or stiff ( $L_p \gg L$ ). A unique property of semi-flexible fibers is strain-stiffening, observed in most of natural tissue fibers, for example in fibrin and collagen (Figure 2F).<sup>57-59</sup> The ability to stiffen as the fibers are being stretched is used to withstand large mechanical loads which could threaten tissue integrity.<sup>60</sup> Strain-stiffening fibrous networks enable long-range force sensing of up to hundreds of microns.<sup>61</sup> Furthermore, strain-stiffening was shown to be crucial for stem cell differentiation, however the mechanism is not clearly understood.<sup>16</sup> On one hand, the strain-stiffening behavior in networks

of semi-flexible filaments originates from entropic elasticity, which produces an opposing force when the filaments are being stretched.<sup>60</sup> On the other hand, the non-linear behavior can be explained by the transition from soft bending modes into a stiffer stretching-dominated regime.<sup>62</sup> Even though strain-stiffening is an invariable property of semi-flexible chains,<sup>60</sup> it can be also induced by mechanically driven crosslinking.<sup>43</sup>

### 3. Macroporous Hydrogels

Most tissues are architected materials with elements such as the vascular porosity or the lacuno-canalicular porosity in bone.<sup>63</sup> Inspired by these natural architectures, bioengineers started using porosity for *in vitro* tissue engineering. The main advantage of macroporous hydrogels is that they promote mass transport necessary for nutrient supply and waste disposal. Depending on the pore size, cell spreading or even cell migration may be facilitated. The nomenclature of different pore sizes has not always been consistent, but Elbert has proposed the following definitions: “Macroporous” for pore diameters larger than 1  $\mu\text{m}$ , “microporous” between 100 nm and 1  $\mu\text{m}$ , and “nanoporous” up to 100 nm.<sup>64</sup> The same definitions will be used throughout this review. Most covalently crosslinked hydrogels are inherently nanoporous.<sup>65</sup>

#### 3.1 Design Considerations

A permissive tissue culture environment must enable cells to access nutrients and remove waste via molecular transport mechanisms. Molecules flow into hydrated gels either by diffusion caused by a concentration gradient, or by convective fluid flow caused by a pressure gradient.<sup>66</sup> Whereas diffusion-driven flow is mostly determined by the intrinsic properties of solute molecules, the permeability of a hydrogel is a measure of resistance to convective fluid flow.<sup>67</sup> Therefore, permeability is an important material property defining the inflow of nutrients into the gel. It is strongly influenced by the pore size of the material. Hydrogels with greater pore or mesh size have greater permeability values, indicating that they exert less resistance to fluid flow and allow for a better nutrient supply than other gels.<sup>67</sup> This correlation was previously described by Moreno-Arotzena et al. and justifies the importance of precisely designed porous architectures within hydrogels.<sup>67</sup> Moreover, delivering interstitial fluid flow within porous structures creates mechanical stimuli, namely fluid shear stress (FSS).<sup>66</sup> The magnitude of FSS depends on the pore size in a 3D scaffold.<sup>68</sup>

#### 3.2 Preparative Methods and Applications

With the design considerations in mind, techniques to create tailored micro- or macroporosity for specific tissue engineering applications are discussed in this section. Four main methodological categories are highlighted: porogen leaching, microgel annealing, phase separation and microstrand processing. An overview can be seen in **Figure 4** and the advantages and disadvantages are listed in **Table 2**.

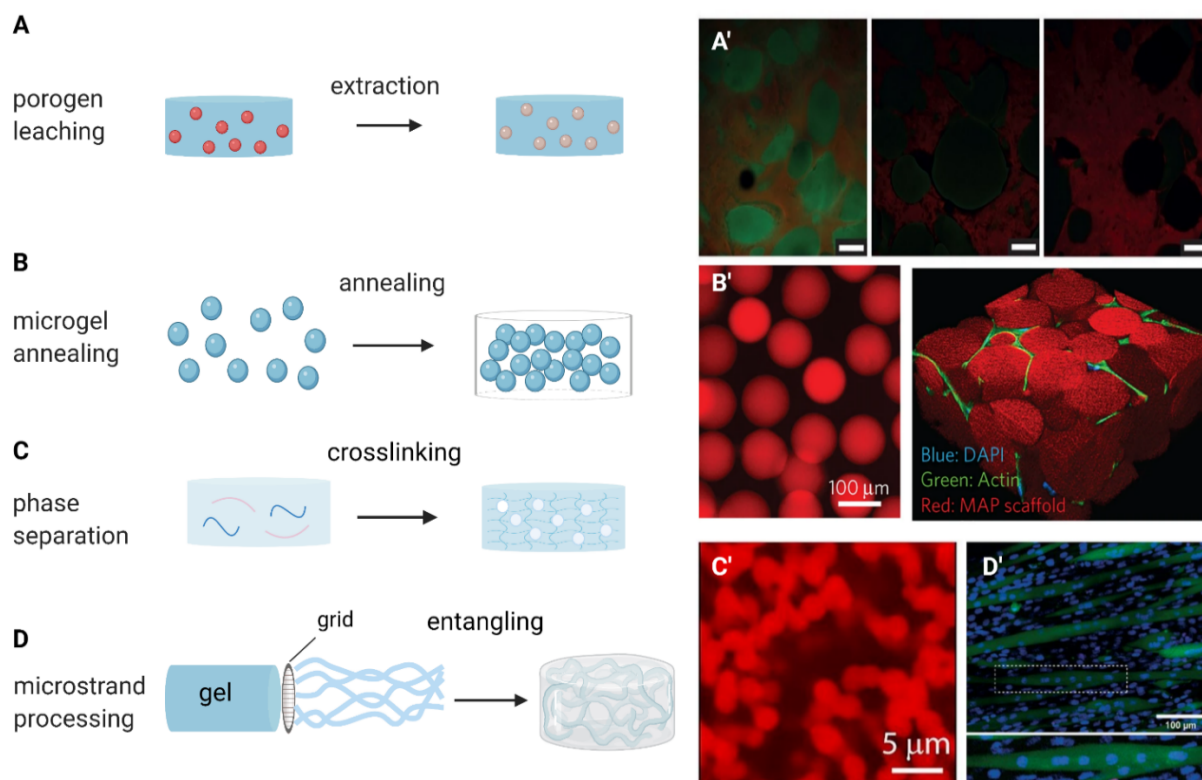


**Figure 4.** Schematic representation of the different methods used to create macroporous hydrogels. **(A)** Porogen leaching, **(B)** microgel annealing, **(C)** phase separation and **(D)** microstrand processing. Figures from primary literature: A' adapted from Ref.<sup>69</sup> with permission of Springer Nature, B' adapted from Ref.<sup>70</sup> with permission of Springer Nature, C' adapted from Ref.<sup>71</sup> with permission from Elsevier, D' adapted from Ref.<sup>12</sup>, licensed under a Creative Commons Attribution License; Illustrations created with BioRender.com. Scale bars: 1 mm (A'), 100 μm (B',D'), 5 μm (C').

**Table 2:** Summary of advantages and disadvantages of different methods for creating macroporous hydrogels.

Methods	Advantages	Disadvantages	References
porogen leaching	+ higher mechanical stability	- harsh conditions (low pH/freeze-drying) during porogen extraction	69, 72-73
microgel annealing	+ injectable + scalable and high degree of control over microgel size	- lower mechanical stability with pores - trade-off of dimension control and up-scalability - closing of pores through gel refusion	70, 74-78
aqueous phase separation	+ in situ gelling + compatible with 3D culture + injectable	- complex composition - long and demanding mixing procedure	71
microstrand processing	+ anisotropic structures + compatible with extrusion printing	- lower porosity - only suitable for soft hydrogels	12, 79-80

### *Porogen Leaching*

Porosity can be generated by encapsulating degradable porogens into a hydrogel. For example, Huebsch et al. have included hydrolytically degradable oxidized alginate gels (~150  $\mu\text{m}$  diameter) as porogens in a bulk alginate gel.<sup>69</sup> This way, bulk gel stiffness and pore formation could be decoupled, and they showed optimal osteogenic lineage commitment of mesenchymal stem cells (MSCs) and bone formation *in vivo*. Colloidal-crystal templating relies on a similar principle. A template of ordered microspheres (20-60  $\mu\text{m}$  diameter) is created and perfused with the gel precursor solution. The microspheres are then removed by solvent extraction after polymerizing the hydrogel. With this method, Stachowiak et al. could produce scaffolds with a lower level of porosity of  $65\% \pm 3\%$  and less decrease in mechanical stability than most other porous hydrogels.<sup>72</sup> The size of the pores connecting the voids created by the microspheres was around 5-15  $\mu\text{m}$  depending on the diameter of the microsphere. Freeze-drying is a method where ice crystals can be considered as the porogens. Upon sublimation, interconnected voids are created across 3D space within the material.<sup>73</sup> At this point, cells are seeded and the hydrogel swells when medium is added. The porosity and pore size decreased from around 93% to 30% and from 280  $\mu\text{m}$  to 54 or 120  $\mu\text{m}$  depending on the solvent with swelling. With this method, homogenous cell seeding into the dried scaffolds was achieved.

### *Microgel Annealing*

Porous hydrogels can also be generated by annealing microgels. In porogen leaching, the porogens commonly leave behind spherical pores. In contrast, commonly spherical microgels are annealed to a scaffold and surrounded by a non-spherical void space in microgel annealing. Microgels can be created with a variety of methods, where there is often a trade-off between high degree of control over the microgel dimensions and simplicity of the method. Microgels of a controllable size could be fabricated for instance using microfluidic devices for generating a water-in-oil emulsions.<sup>70, 74</sup> Other microfluidic fabrication techniques for microgels are summarized elsewhere.<sup>81</sup> Before removing the oil, the microgels are crosslinked. Griffin et al. crosslinked poly(ethylene) glycol vinyl sulfone (PEG-VS) gels by Michael-type addition using a degradable crosslinker enabling cells to further remodel the matrix. The PEG-VS microgels were then enzymatically annealed, so that the microgels could also be injected before annealing. The pore diameter was in the range of 10 to 35  $\mu\text{m}$ . They showed accelerated wound closure using these microgel annealed hydrogels.<sup>70</sup> By injecting a very similar hydrogel with hyaluronic acid as the backbone, neural progenitor cells were promoted to migrate to a site affected by stroke in a mouse model.<sup>75</sup> Later, Sheikhi et al. developed a more straightforward method, namely physical crosslinking of gelatin methacrylate (GelMA) by cooling it to 4°C.<sup>74</sup> The GelMA gels were then annealed using ultraviolet light to form a macroporous hydrogel (~20  $\mu\text{m}$  pore diameter). With this method, infiltration of human umbilical vein endothelial cells (HUVECs) could be accelerated compared to bulk GelMA hydrogels. Gehlen et al. developed an even simpler method. They created gel granules by pushing a cellulose nanofibril hydrogel through a nylon mesh

and annealed the granules by the addition of cell culture medium. They achieved increased fibroblast spreading but only minimal to incomplete cell infiltration, which they attribute to the fusion of the hydrogel after meshing.<sup>76</sup>

#### *Aqueous Phase Separation*

Aqueous polymer-polymer phase separation is another phenomenon that can be used to form pores. The most common materials for this are PEG with another polymer such as dextran or a salt. The reader is hereby referred to a review about phase separation for the creation of porous hydrogels.<sup>64</sup> The advantage of this method is that pore formation can occur *in situ*, which allows for a more uniform cell distribution. Recently, Broguiere et al. used this technique to generate neural networks from a Michael-addition type hydrogel based on PEG-VS in combination with polysaccharides such as hyaluronan.<sup>71</sup> They suspended dorsal root ganglia as well as rodent neurons in a hydrogel precursor mixture which phase separates upon polymerization to form pores in the micro- and macroporous range (0.5 – 50  $\mu\text{m}$ ). Increased axon growth was observed when implanting the porous gel in a mouse with a damaged sciatic nerve. However, the disadvantages of this method are the rather long gelation time, and the complexity of the phase-separating mixture. Gelation time could be reduced by using a more efficient crosslinking mechanism such as thiol-ene photopolymerization. With such a mechanism, phase separation could be combined with light-based 3D printing, so that multiscale architected materials could be generated. To date, reports on photoinitiated PIPS<sup>82</sup> are scarce. Nevertheless, future developments of photosensitive hydrogels for PIPS are extremely promising for 3D printing of porous scaffolds or medical devices

#### *Microstrand Processing*

The porous hydrogels discussed so far were all isotropic, and thus do not resemble most human tissues, especially musculoskeletal ones. Microstrands or high-aspect-ratio microgels have been explored for creating anisotropic porous hydrogels, which provide guidance cues for cells such as neurons.<sup>79-80</sup> Recently, simple fabrication of microstrands by pushing a bulk gel through a grid had been developed and was shown to be suitable for extrusion-based bioprinting.<sup>12</sup> In fact, the strands were aligned during printing allowing for further control of the structure of the hydrogel. This is especially promising for engineering larger scaffolds. The pore fraction was in the range of 5% while the pore size was not analyzed.

## **4. Architected Hydrogels by 3D Printing**

Although fibrillar and macroporous hydrogels are advantageous for mass transport and cell migration inside a 3D environment compared to traditional non-structured hydrogels, a major drawback is that the exact arrangement and interconnectivity of the pores are not controllable. This is where digital 3D printing techniques can be used to fabricate tissues with a more user-defined internal architecture. For instance, the

fabrication of vasculature can be realized through biomimetic 3D printing in accordance with medical imaging data in the presence of living cells. This section provides an overview of approaches to create more user-defined architectural features within hydrogels by means of high-resolution light-based 3D-printing methods.<sup>83</sup> **Table 3** summarizes a list of these techniques that have shown promise for creating functional architected hydrogels. According to the manufacturing principle, these techniques can be classified into additive manufacturing (AM) and subtractive manufacturing.

**Table 3:** Summary of the advantages and disadvantages of different 3D printing techniques for creating architected hydrogels.

Techniques	Wavelength (nm)	Resolution (nm)	Advantages	Disadvantages	References
Stereolithography	405-500	2000 - 8000	+ fabrication time of a few minutes + compatibility with cell printing	- resolution limit ca. 50 $\mu\text{m}$ - layer-by-layer process	84-85
Two-photon polymerization	700-1000	200 - 2000	+ submicron resolution + user-defined architecture	- lack of highly reactive and cell-friendly gels - long fabrication time	86-90
Two-photon laser ablation	700-1000	500 – 1000	+ submicron resolution + ability to create guidance microchannels	- high laser dosage - potential cellular damage - long fabrication time	91-92

#### 4.1 Additive Manufacturing

AM techniques have expanded substantially in recent years for a variety of applications in the biomedical field. Among these techniques, extrusion-based 3D bioprinting remains the mainstream technique to create a centimetre-scale tissue construct. This technique generally requires a shear-thinning bioink that can be extruded as a filament through a nozzle. Although it is compatible with multiple materials and various cell types, the major drawback is the limited printing resolution (150-500  $\mu\text{m}$ ).<sup>93</sup> Therefore, when it comes to printing anatomically shaped 3D structures, light-based 3D printing methods<sup>94-95</sup> are highly desirable.

##### *Stereolithography*

Stereolithography (STL) is an AM technique that uses a photochemical process to cure the resin in a layer-by-layer fashion. One main challenge in STL is the development of a hydrogel bio-resin that is photocrosslinkable and cell-compatible while exhibiting suitable light absorbance and viscosity. Grigoryan et al. recently developed a resin composed of PEG di-acrylates and food additives as the absorber for

printing functional tissues with complex network architectures (**Figure 5A**). The authors firstly demonstrated the fabrication of intertwined vascular networks and then proceeded with the fabrication of an alveoli model which could be perfused with red blood cells. Furthermore, this technique was used to print a vascularized hepatic hydrogel scaffold that could be perfused and seeded with endothelial cells after printing.<sup>84</sup> The big advantage of STL is that hydrogels can be printed within minutes, showing an advantage for scaled fabrication.<sup>84</sup> Using a GelMA resin, a dynamic optical projection STL technique was developed to fabricate vascular-like hydrogel constructs comprising living cells with a viability of 75%.<sup>96</sup> Although the fabrication time is desirable, the resolution is still limited to a voxel size of 50  $\mu\text{m}$ .<sup>84</sup>

### *Two-Photon Polymerization*

To 3D print an architected hydrogel at submicron-scale resolution, two-photon polymerization (2PP) is one of the most promising methods. In 2PP, a femtosecond-pulsed near-infrared laser is used to locally solidify photopolymers, which enables the fabrication of structural features down to 65 nm.<sup>97</sup> The underlying principle of 2PP is the simultaneous absorption of two photons by a photoinitiator that leads to the excitation of the initiator and the crosslinking only at the focal spot. Conventional resins developed for UV polymerization are not processable by 2PP due to poor photo-reactivity, whereas low  $M_w$  acrylates are acutely cytotoxic. To address these limits, Liska and co-workers recently reported low toxic hydrogels based on vinyl ester derivatives of gelatin and hyaluronan.<sup>87-89</sup> Qin et al. reported the first cell-instructive photo-clickable hydrogel based on protease-sensitive polyvinyl alcohol (PVA) matrices that permit cell-matrix remodelling, cell invasion, multicellular self-organization and ultrafast 2PP fabrication at speeds up to 50 mm/s.<sup>86</sup> A 3D architected scaffold mimicking the liver lobule was fabricated by 2PP of PVA hydrogels (**Figure 5B**). Furthermore, it was demonstrated that a multiphoton laser could be used to attach extracellular cues to a specific site within the hydrogel, leading to light-guided cell migration (**Figure 5C**). The spatial resolution achieved was at micrometer-scale.<sup>86</sup>

## **4.2 Subtractive Manufacturing**

While AM techniques are widely sought to fabricate architected hydrogels, subtractive manufacturing techniques have emerged as new tools to create functional hollow structures in a more efficient fashion. For instance, AM of a 3D hydrogel construct containing a vascular network by 2PP may take up to hours or days, which is 10 times longer than the time required for a subtractive process. For the fabrication of vasculature and other porous structures (e.g., the lacuno-canalicular network), subtractive manufacturing by means of light-induced material erosion or degradation holds the potential to revolutionize the field of tissue engineering.

### Two-Photon Laser Ablation

Two-photon-induced hydrogel degradation is extremely useful for the creation of defined channel architectures to guide cell outgrowth and tissue development. Since two-photon hydrogel patterning offers high spatial resolution, several research groups worldwide have employed two-photon laser ablation to control cell growth in a spatially and temporally controlled fashion.<sup>91, 98-100</sup> A seminal study by Sarig-Nadir et al. demonstrated laser-guided outgrowth of dorsal root ganglia cells into photoablated channels, showing that the ablation process is compatible with 3D cell culture.<sup>91</sup> Moreover, it allows for more detailed studies on the interaction of cells with architectural features in the printed niche. However, direct laser exposure to a cell and resultant damage remains a concern. Arakawa et al.<sup>92</sup> used two-photon laser ablation to print perfusable capillary microchannels in a collagen hydrogel to guide the formation of robust 3D microvessels (Figure 5D). With this powerful approach, it is possible to design high-resolution capillary networks within hydrogels according to a predefined design. Moreover, it enables researchers to systematically investigate the effect of geometric and mechanical cues on cell activity during cell culture at high spatial resolution. Therefore, one application of this method could be to spatiotemporally guide the sprouting of vessels and assess the cellular guidance effect in close vicinity. The main advantage of laser ablation is the ease of integrating user-defined designs. Clinical imaging data as well as architectures illustrated in computer-aided design (CAD) software can be used to generate a mask for the ablation of the depicted pattern into the hydrogel.<sup>98-99</sup> However, one drawback is the long fabrication time. So far, this technique needs approximately 1.4 hours to degrade structures within a 0.014 mm<sup>3</sup> hydrogel.<sup>101</sup>

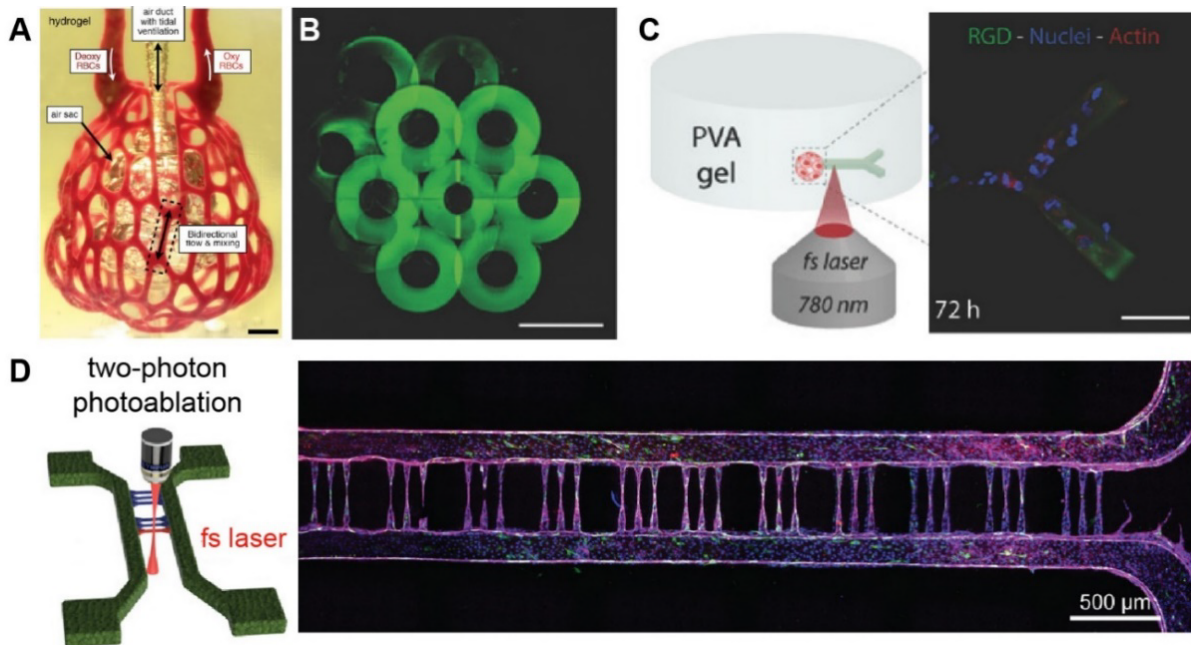


**Figure 5.** Light-based 3D printing technologies and applications. (A) Stereolithography: Intricate and functional vascular architectures were printed within cell-compatible hydrogels. Photograph of a printed hydrogel containing the

distal lung subunit during red blood cell perfusion while the air sac was ventilated with O<sub>2</sub>. Scale bar = 1 mm). Adapted from Ref.<sup>84</sup> with permission of Science. **(B)** Two-photon polymerization (2PP): 3D layered tissue-mimicking scaffold printed by ultrafast 2PP of polyvinyl alcohol (PVA) hydrogels. **(C)** Two-photon micropatterning: biochemical cues were site-specifically immobilized inside a 3D PVA matrix, allowing laser-guided cell growth. Scale bars = 100 μm. (B) and (C) adapted from Ref.<sup>86</sup> with permission from WILEY. **(D)** Two-photon laser ablation: guided capillary outgrowth in lithography-based microvessel devices. Confocal image of a complete vessel network consisting of 33 capillaries. Green: von Willebrand factor; blue: nuclei; red: VE-cadherin; purple: F-actin. Scale bar = 500 μm. Adapted from Ref.<sup>92</sup> with permission of Science.

## 5. Emerging applications for Architected Hydrogels

Architected hydrogels have become a valuable tool not only for tissue engineering, but also to study the interaction of cells with their environment for both basic and translational research in biomedicine. The following section aims to review emerging applications of these materials for tissue engineering, for instance, in combination with microfluidics to engineer ‘organ-on-a-chip’ systems, and highlights how these materials have been utilized for functional tissue engineering and mechanobiological studies.

### 5.1 Microfluidic 3D Culture

In the last decade, microfluidic technology has found various applications in the biomedical field, especially in tissue engineering in the form of ‘organs-on-a-chip’. These tools provide control over environmental cues, mechanical stimuli, and cell-matrix interactions. In contrast to 3D cell culture in bioreactors, fewer cells and reagents are needed and they enable real-time analysis of biochemical markers as well as high-resolution image acquisition. Given these advantages, such microfluidic systems are especially valuable to model tissues and organs for drug discovery and development.<sup>102</sup> The application of microfluidic chips for 3D cell culture has become valuable to provide more physiologically relevant mechanical cues to cells compared to static culture. The technique allows not only for the integration and specific spatial arrangement of various cell types into tissue models like in the lung-on-a-chip developed by Huh et al.<sup>103</sup>, but also for the application of FSS that can influence cell alignment and tissue maturation.<sup>104-107</sup> Further, stable chemical gradients can be generated by diffusion due to the laminar flow regime inside the microchannels.<sup>108</sup> Integration of 3D architected biomaterials in microfluidic devices offers great potential to obtain *in vitro* tissue and organ models that mimic such environmental cues that are presented to cells *in vivo* (**Figure 6A**).<sup>109</sup> These cues include stiffness, porosity, chemical composition, adhesion sites, architecture and dynamic properties of the material such as swelling or degradation.<sup>110</sup> These properties can be tailored according to the specific type of tissue or organ to be modeled. For instance, defined porosity influences the materials permeability and thereby the FSS acting on cells in 3D dynamic culture. Furthermore, transport of nutrient and waste products is facilitated by larger permeability. The combination of architected materials and microfluidic technology therefore provides many advantages over traditional 3D cell culture. Studies that exploited these benefits are highlighted in this section.

Natural fibrillar hydrogels are frequently incorporated in microfluidic cell culture. Park et al. developed an injection molded plastic array device with collagen as the ECM to culture lymphocytes and cancer cells for assessing the killing abilities of cytotoxic lymphocytes in a 3D environment.<sup>111</sup> Others quantified 3D chemotaxis in microfluidic-based chips with gradients of collagen hydrogel concentrations.<sup>112</sup> Takehara et al.<sup>113</sup> used fibrin in a microfluidic vascular-bed device for vascularized tissue engineering. Further, stable collagen microgels with aligned microstructure were achieved using flow-driven co-deposition.<sup>114</sup>

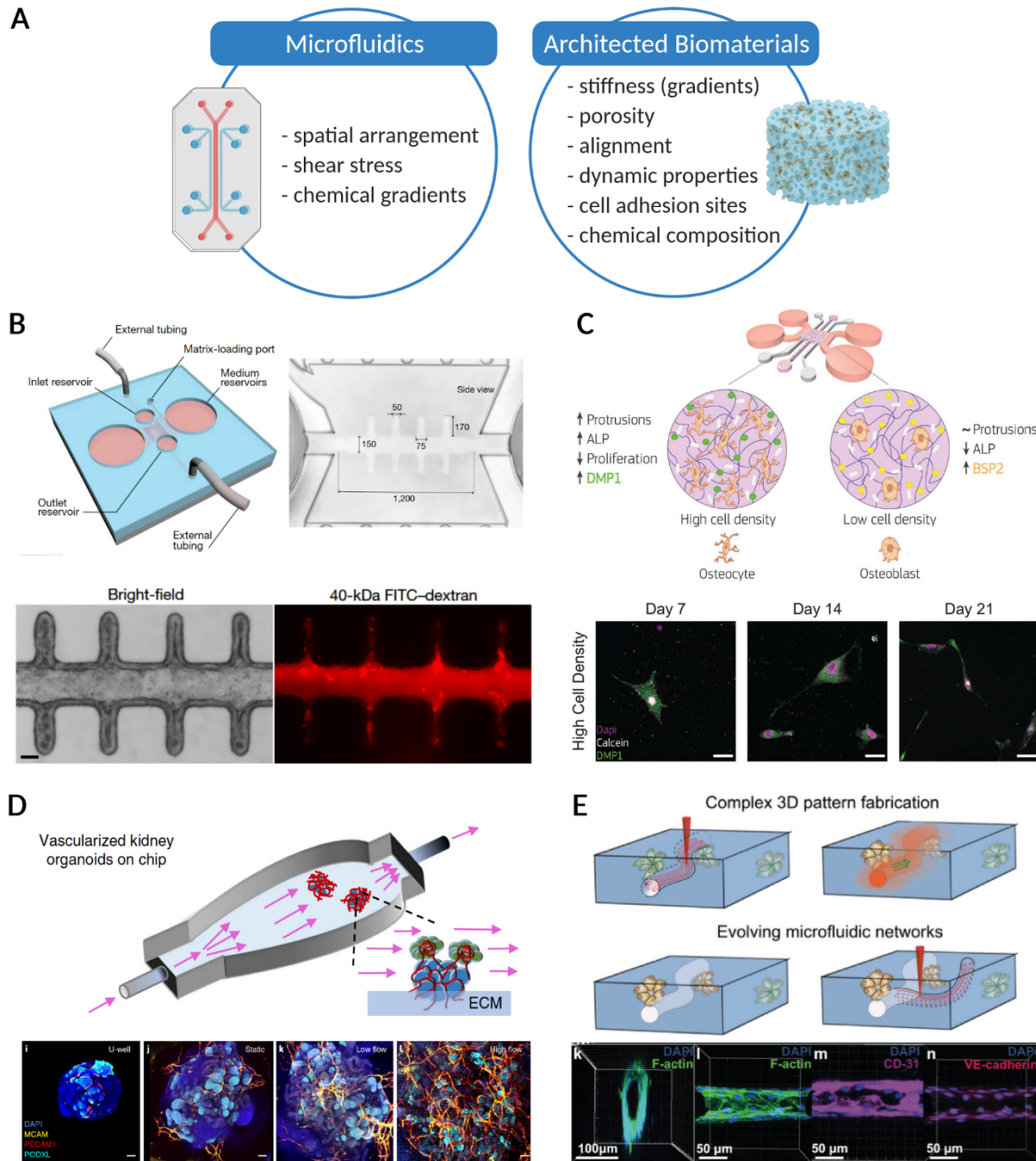


**Figure 6.** Application of architected biomaterials for microfluidic cell culture. **(A)** Properties of microfluidic culture and architected biomaterials that influence cell and tissue behavior. **(B)** Microfluidic culture of perfusable tubular gut organoids. Top: Schematic of 3D hydrogel containing microdevice and channel dimensions, bottom: confocal images of 5-day-old organoid perfused with fluorescein isothiocyanate (FITC)-dextran showing maintenance of gut

epithelium. Scale bar = 50  $\mu\text{m}$ . Adapted from Ref.<sup>115</sup> with permission of Springer Nature. **(C)** Osteoblast maturation towards osteocytes on microfluidic device without flow. Top: setup and maturation of osteoblasts cultured at high cell density, bottom: secretion of DMP1 in cells cultured at high density. Scale bars = 30  $\mu\text{m}$ . Adapted from Ref.<sup>116</sup>, licensed under a Creative Commons Attribution License. **(D)** Enhanced vascularization of kidney organoids upon application of fluid shear stress (FSS) during nephrogenesis. Top: schematic of millifluidic setup, bottom: confocal 3D renderings for vascular markers in whole-mount organoids cultured under static U-well, static engineered ECM, low-FSS, and high-FSS conditions. Scale bars = 100  $\mu\text{m}$ . Adapted from Ref.<sup>117</sup> with permission of Springer Nature. **(E)** Schematic depiction of fabrication and use of *in situ* biomicrofluidics using the ablative properties of focalized nano- or femto-pulsed lasers. Top: illustration of the fabrication process, bottom: confocal 3D reconstruction of a hollow cell tube formed in collagen showing CD-31 markers. Adapted from Ref.<sup>98</sup> with permission from WILEY. Created with Biorender.com.

Another example for an architected biomaterial used in microfluidic 3D culture is microfluidic hydrogel. It can be fabricated by molding (either with microneedle or fiber templates), soft lithography, bioprinting or photopatterning and the obtained microchannels can be directly perfused using different types of pumps.<sup>118</sup> Hydrogels can also be casted into pre-made microfluidic devices fabricated by soft lithography. In this case, the flow is applied to the microfluidic channels on the chip. Moreover, electrospinning can be employed to obtain micro-architected biomaterials within microfluidic channels, either by directly spinning the polymeric fibers into the microchannels or by modular integration of fibers into the chip. This technology holds great potential for the application in organ-on-a-chip systems.<sup>119</sup>

## 5.2 Intestinal Organoids-on-Chip

Combinations of architected hydrogels with microfluidics can not only be used to apply physiologically relevant environmental cues to cultivated cells, but also to improve reproducibility and reduce heterogeneity of organoid culture and to allow for automated real-time analysis. For instance, Brandenburg et al.<sup>120</sup> developed molded hydrogel microcavity arrays to culture individual patient-derived colorectal cancer organoids to screen for anticancer drug candidates. In another study by Nikolaev et al.<sup>115</sup>, the authors induced intestinal stem cells to form perfusable tube-shaped epithelia on chip with similar spatial arrangement as *in vivo* using a collagen I and Matrigel matrix. Applying fluid flow to this system via an external pump prolonged tissue lifespan, enhanced regenerative capacity and allowed the authors to model tissue-microorganism interactions (Figure 6B). These two examples highlight different ways how microfluidics and architected hydrogels can be integrated to improve throughput, reproducibility, and physiologically relevant culture conditions for intestinal organoids.

## 5.3 Bone Tissue Engineering

In bone tissue engineering, one important challenge is the creation of dynamic microfluidic 3D culture models of mature bone cells (osteocytes). Gu et al.<sup>121</sup> sought to reconstruct a 3D osteocyte network in a dynamic culture. For this, they used a scaffold made of biphasic calcium phosphate microbeads in which murine early osteocytes were seeded and cultured in a microfluidic chamber. The porosity of the framework

enabled embedded cells to form a 3D cellular network and to produce mineralized extracellular matrix to fill up the interstitial space. A recent study by Nasello et al.<sup>116</sup> reported the development of a functional unit to achieve osteoblast maturation toward osteocytes and matrix mineralization (Figure 6C). Primary human osteoblasts were suspended in a solution containing collagen I which was then casted into a microfluidic Polydimethylsiloxane (PDMS) chip fabricated by soft lithography. The authors could show that osteoblasts differentiated into osteocytes, expressing cell-type specific markers such as dentin matrix acidic phosphoprotein 1 (DMP1) and alkaline phosphatase (ALP) when cultured at a high cell density of  $1 \times 10^6$  ml<sup>-1</sup> in this 3D environment without the application of flow. The combination of physiologically relevant FSS and architected microenvironment in such a device holds great potential to further facilitate differentiation of less mature osteocyte progenitors such as mesenchymal stem cells. Both studies indicate that not only spatial cues, but also the mechanical environment can promote cell and tissue maturation and thereby highlight the relevance of further investigation of integration of architected biomaterials and microfluidics.

#### **5.4 Neural/muscle Tissue Engineering**

Novel methods for the fabrication of architected hydrogels will allow for the preparation of even more *in-vivo*-like tissue models. An example of models that have profited from the use of architected hydrogels are electro-excitable neural or muscle tissues. Nih et al. injected microgels into tissue sites where stroke occurred and were first to show migration of neural progenitor cells to the affected area. Inflammation and the scar size were decreased, while vascularization in the surrounding area was increased. Only little blood vessel infiltration into the hydrogel was observed.<sup>75</sup> For muscle tissue engineering, Kessel et al. reported an elegant method for the alignment of myotubes using entangled hydrogel microstrands.<sup>12</sup> In this study, myoblasts were embedded in a bulk hydrogel and subsequently sized into microstrands through extrusion. The void space between microstrands led to rapid tissue maturation.

#### **5.5 Engineered Vascular Networks**

Insufficient vascularization of 3D organoids is a limitation that many researchers face when using traditional static culture methods. The enhancement of this process during *in vitro* culture is therefore extensively pursued. It has been shown that the application of FSS using a millifluidic perfusion device enhances vascularization of kidney organoids cultured atop of a gelatin-fibrin matrix (Figure 6D).<sup>117</sup> Recently, Zohar et al.<sup>122</sup> used a similar approach to achieve vascularization, but translated the model into 3D by utilizing porogen leaching to obtain a porous scaffold made from poly-L-lactic acid (PLLA) and poly-L-glycolic acid (PLGA). Endothelial cells and fibroblasts were then cultured inside the construct under various flow conditions using a perfusion bioreactor. Enhanced vascular network morphogenesis and higher

colocalization of alpha-smooth muscle actin ( $\alpha$ -SMA) with endothelial vessel networks were observed compared to a static control culture.

A method to design a vascular network inside a hydrogel was described by Brandenberg et al.<sup>98</sup> They used laser-based photoablation to obtain a 3D system of channels inside a collagen I hydrogel that was subsequently seeded with endothelial cells by microfluidic perfusion to obtain a mature perfusable vascular network after five days of culture (Figure 6E). Baker et al.<sup>123</sup> were further able to generate temporally and spatially defined gradients of diffusive molecules by patterning microfluidic channels in a 3D ECM using micromolding. They showed that cell populations can be cultured independently either within the channels or the surrounding ECM. When lining the generated microchannels with endothelial cells, the authors found that varying channel architecture and thereby diffusion patterns guides location and morphology of endothelial sprouting. These methods will become valuable tools to tackle the obstacle of insufficient or non-perfusable vasculature of organoids and tissue culture models.

## 5.6 Mechanobiology

It is appreciated that mechanical cues in a 3D culture environment have a strong impact on cell fate (differentiation, mechanotransduction, apoptosis).<sup>86, 124-126</sup> Although non-architected hydrogels were used for 3D mechanobiological studies, they are not able to resemble physiological relevant microstructures in native tissues. The promise of architected hydrogels lies in the presentation of architectural cues and the compatibility to introduce fluid flow through either the pores or engineered channels to the hydrogel. This offers a simple but powerful tool for 3D mechanobiological studies and for understanding the mechanisms of flow-induced cellular mechanosensation and signal transduction.

Increasing attention has been devoted to incorporating mechanical cues into a 3D cellular environment. For instance, the integration of perfusable network structures will allow one to deliver fluid flow to the cells embedded in a hydrogel. Mei et al. studied the effect of breast cancer extravasation on bone remodelling by creating a microfluidic bone model.<sup>127</sup> It was shown that oscillatory fluid flow caused a 3.7-fold higher intracellular calcium response in osteocytes compared to non-stimulated control. Moreover, mechanical stimulation also resulted in an effective reduction of cancer cell extravasation into hydrogel-filled side channels. This highlights the important role of bone fluid flow in the mechano-regulation of osteocytes to prevent cancer metastasis, although the mechanism still needs to be elucidated. In another study using a microfluidic setup as a lymphatic *in vitro* model, Lee et al. showed that wall shear stress leads to nuclear localization of TAZ in prostate cancer cells.<sup>128</sup> Moreover, it was found that this nuclear translocation increased proliferation of the prostate cells. These findings suggest that the fluid forces in lymphatic vessels are an important trigger for the proliferation of prostate cancer cells.

The influence of architected hydrogels with a fibrillar structure on cellular morphology was studied by Baker et al.<sup>129</sup> The group developed a fibrillar hydrogel made of methacrylated dextran, which allowed for

precise control of parameters like fiber thickness, alignment, density and stiffness. When cells were exposed to softer fibers, not only active recruitment of fibers but also more focal adhesion sites as well as increased phosphorylation of focal adhesion kinases were observed, highlighting the influence of fiber stiffness on cell behavior. Focal adhesion kinases are transducers of cellular adhesion via mechanobiological signaling pathways. Here, increased proliferation and spreading were observed in scaffolds with soft fibers compared to stiffer fibers. The influence of FSS on cell migration and focal adhesion proteins was also observed by Polacheck et al.<sup>130</sup> By engineering a tumor-associated model of interstitial fluid flow within a microfluidic device, they showed that fluid flow can induce polarization in cells that are embedded in a collagen type I hydrogel. Both studies show that cell migration and proliferation are initiated not only intrinsically by the cells but are also extrinsically stimulated by their surrounding mechanical environment.

The fabrication of internal architectures allows researchers to not only consider the mechanics of the scaffolding material but also multiple other biophysical cues such as fiber dimensions, curvature, and fluid flow on cellular mechanosensation and signal transduction. Combining architected hydrogels with 3D cell culture and biomechanical stimulation is a highly challenging but necessary step to fabricate more *in vivo*-like tissue models for a variety of cutting-edge applications in regenerative medicine.

## 6. Summary and Future Outlooks

When it comes to culturing cells in a 3D environment or engineering a functional tissue construct, researchers have been taking lessons from nature over the past years. Novel architected materials – of natural and synthetic origin - and techniques to fabricate them have been developed to better replicate native tissue structure which is directly linked to tissue function. Fibrillar hydrogels, for example, more closely resemble the architecture of the native ECM than traditional synthetic hydrogels, and mimic some of the tissue's mechanical properties such as strain-stiffening. Capturing this cell-relevant feature in a synthetic system was achieved and studied in a couple of recent developments. However, the hydrogels still require further improvements in terms of permissiveness and biodegradability which are necessary in most of 3D cell culture and tissue engineering applications.

One way to improve the permissiveness for cells within an engineered scaffold is to use macroporous hydrogels. We reviewed several methods to design and fabricate such architectures within hydrogels in this article. Despite important progress, several challenges remain to be addressed. Firstly, many methods are difficult to scale up, especially in the case of highly controlled porosity. This aspect has been partially addressed by Kessel et al. by using grids with a mesh size of 40–100  $\mu\text{m}$ .<sup>12</sup> The fast and easy process created entangled microstrands with interconnected void spaces that could facilitate the formation of aligned myotubes. This illustrated that macroporous hydrogels can be produced at greater scales by an easy process which is applicable to different types of hydrogels. Another challenge is the mechanical stability in macroporous hydrogels which is often reduced due to the high porosity needed for

interconnectivity. Two approaches to reduce the porosity are highly ordered porogens or phase separation producing elongated instead of spherical pores.<sup>71-72</sup> The use of one of these methods possibly in combination with mechanically stable bulk hydrogel is recommended in applications which require high mechanical stability. For clinical use, a variety of methods would be suitable for injection so that minimally invasive deployment of the hydrogel *in vivo* is foreseeable.<sup>69-71, 74-75, 79-80</sup> To control the macroscopic shape of porous tissue engineered constructs, 3D printing could be employed, for example by combining microstrands and extrusion bioprinting<sup>12</sup> or light-based 3D printing with phase separation.

Recent years have witnessed encouraging progress in 3D printing of architected hydrogels across scales. Technological developments in STL, 2PP and two-photon laser ablation have made up a multiscale engineering toolbox in dealing with the interdisciplinary challenge for scaled fabrication at high spatial resolution when compared to extrusion-based printing or electrospinning. Future research will most likely focus on improving the throughput of these techniques by increasing the printing speed with the help of more efficient photopolymers. This is crucial to future developments towards precision organ-on-chip models and intelligent biosystems, which combine a resolution down to micron-size, ease of fabrication, online monitoring and biocompatibility.

In this review article, we highlighted a variety of emerging applications for architected hydrogels, for example in microfluidic 3D culture, functional tissue engineering and mechanobiology. Among them, a very promising approach to replicate native tissue environments is to combine these designer materials with mechanical stimulation to provide further essential cues to cultured cells. The integration of architected biomaterials with microfluidics is already implemented in various fields of research as we reviewed in this article. Additionally, these tools have been implemented in stem cell engineering, drug screening, replicating tissue-tissue interfaces, reproducing parenchymal tissues and various other organ-on-a-chip systems as well as tumor cell mechanobiology and will most likely become even more important in the future.<sup>109, 131-133</sup> However, there are challenges that remain to be addressed. For instance, PDMS is known to absorb small molecules which limits the application of microfluidic 3D cultures, especially in the pharmaceutical area.<sup>132</sup> Furthermore, in most cases, expensive equipment and expertise in techniques like lithography are required for the fabrication of such on-chip systems. To make this technology more accessible for various research applications, it is therefore necessary to find methods to either simplify the fabrication process or to make microfluidic 3D cultures commercially available. Standardization of protocols for hydrogel preparation and flow control could, moreover, lead to highly reproducible cell culture conditions within this microfluidic 3D environment.

Altogether, recent advances in biomaterials science and 3D printing described in this article have enabled researchers to design and fabricate complex hydrogel scaffolds with well-defined architectures for growing multicellular structures within static and dynamic 3D environments. Since they better mimic spatial cues presented in natural tissue architectures compared to unstructured scaffolds, these novel materials impact

cell fate such as proliferation, differentiation, or migration – and thereby tissue function. Despite remaining challenges, these architected hydrogels therefore represent a promising tool for future applications in functional tissue engineering and 3D cell culture.

### Acknowledgements

The authors would like to thank ETH Zurich for financial support to a Career Seed Award (SEED-21 18-2). We are grateful to the Swiss National Science Foundation for project funding (Spark Award no. CRSK-2\_190345 and no. 200021\_188522).

### Conflict of Interest

The authors declare no conflict of interest.

### References

1. Fritton, S. P.; Weinbaum, S., Fluid and Solute Transport in Bone: Flow-Induced Mechanotransduction. *Annu Rev Fluid Mech* **2009**, *41*, 347-374.
2. Schneider, P.; Meier, M.; Wepf, R.; Muller, R., Towards quantitative 3D imaging of the osteocyte lacuno-canalicular network. *Bone* **2010**, *47* (5), 848-58.
3. Wisdom, K. M.; Delp, S. L.; Kuhl, E., Use it or lose it: multiscale skeletal muscle adaptation to mechanical stimuli. *Biomechanics and Modeling in Mechanobiology* **2015**, *14* (2), 195-215.
4. Screen, H. R. C.; Berk, D. E.; Kadler, K. E.; Ramirez, F.; Young, M. F., Tendon Functional Extracellular Matrix. *Journal of Orthopaedic Research* **2015**, *33* (6), 793-799.
5. Gracey, E.; Burssens, A.; Cambré, I.; Schett, G.; Lories, R.; McInnes, I. B.; Asahara, H.; Elewaut, D., Tendon and ligament mechanical loading in the pathogenesis of inflammatory arthritis. *Nature Reviews Rheumatology* **2020**, *16* (4), 193-207.
6. Bramson, M. T. K.; Van Houten, S. K.; Corr, D. T., Mechanobiology in Tendon, Ligament, and Skeletal Muscle Tissue Engineering. *Journal of Biomechanical Engineering* **2021**, *143* (7).
7. Kamm, R. D.; Bashir, R.; Arora, N.; Dar, R. D.; Gillette, M. U.; Griffith, L. G.; Kemp, M. L.; Kinlaw, K.; Levin, M.; Martin, A. C.; McDevitt, T. C.; Nerem, R. M.; Powers, M. J.; Saif, T. A.; Sharpe, J.; Takayama, S.; Takeuchi, S.; Weiss, R.; Ye, K.; Yevick, H. G.; Zaman, M. H., Perspective: The promise of multi-cellular engineered living systems. *APL Bioeng* **2018**, *2* (4), 040901.
8. Garreta, E.; Kamm, R. D.; Chuva de Sousa Lopes, S. M.; Lancaster, M. A.; Weiss, R.; Treppe, X.; Hyun, I.; Montserrat, N., Rethinking organoid technology through bioengineering. *Nature Materials* **2021**, *20* (2), 145-155.
9. van Tol, A. F.; Roschger, A.; Repp, F.; Chen, J.; Roschger, P.; Berzlanovich, A.; Gruber, G. M.; Fratzl, P.; Weinkamer, R., Network architecture strongly influences the fluid flow pattern through the lacunocanalicular network in human osteons. *Biomechanics and Modeling in Mechanobiology* **2020**, *19* (3), 823-840.
10. Zhang, J.; Wehrle, E.; Adamek, P.; Paul, G. R.; Qin, X.-H.; Rubert, M.; Müller, R., Optimization of mechanical stiffness and cell density of 3D bioprinted cell-laden scaffolds improves extracellular matrix mineralization and cellular organization for bone tissue engineering. *Acta Biomater* **2020**, *114*, 307-322.
11. McDermott, A. M.; Herberg, S.; Mason, D. E.; Collins, J. M.; Pearson, H. B.; Dawahare, J. H.; Tang, R.; Patwa, A. N.; Grinstaff, M. W.; Kelly, D. J.; Alsberg, E.; Boerckel, J. D., Recapitulating

- bone development through engineered mesenchymal condensations and mechanical cues for tissue regeneration. *Science Translational Medicine* **2019**, *11* (495).
12. Kessel, B.; Lee, M.; Bonato, A.; Tinguely, Y.; Tosoratti, E.; Zenobi-Wong, M., 3D Bioprinting of Macroporous Materials Based on Entangled Hydrogel Microstrands. *Advanced Science* **2020**, *7* (18), 2001419.
  13. Homan, K. A.; Gupta, N.; Kroll, K. T.; Kolesky, D. B.; Skylar-Scott, M.; Miyoshi, T.; Mau, D.; Valerius, M. T.; Ferrante, T.; Bonventre, J. V.; Lewis, J. A.; Morizane, R., Flow-enhanced vascularization and maturation of kidney organoids in vitro. *Nat Methods* **2019**, *16* (3), 255-262.
  14. Zhang, B.; Korolj, A.; Lai, B. F. L.; Radisic, M., Advances in organ-on-a-chip engineering. *Nature Reviews Materials* **2018**, *3* (8), 257-278.
  15. Kouwer, P. H. J.; Koepf, M.; Le Sage, V. A. A.; Jaspers, M.; Van Buul, A. M.; Eksteen-Akeroyd, Z. H.; Woltinge, T.; Schwartz, E.; Kitto, H. J.; Hoogenboom, R.; Picken, S. J.; Nolte, R. J. M.; Mendes, E.; Rowan, A. E., Responsive biomimetic networks from polyisocyanopeptide hydrogels. *Nature* **2013**.
  16. Das, R. K.; Gocheva, V.; Hammink, R.; Zouani, O. F.; Rowan, A. E., Stress-stiffening-mediated stem-cell commitment switch in soft responsive hydrogels. *Nature Materials* **2016**, *15* (3), 318-325.
  17. Han, E.; Chen, S. S.; Klisch, S. M.; Sah, R. L., Contribution of proteoglycan osmotic swelling pressure to the compressive properties of articular cartilage. *Biophysical Journal* **2011**, *101* (4), 916-924.
  18. Bella, J., Collagen structure: New tricks from a very old dog. *Biochemical Journal* **2016**, *473* (8), 1001-1025.
  19. Inzana, J. A.; Olvera, D.; Fuller, S. M.; Kelly, J. P.; Graeve, O. A.; Schwarz, E. M.; Kates, S. L.; Awad, H. A., 3D printing of composite calcium phosphate and collagen scaffolds for bone regeneration. *Biomaterials* **2014**, *35* (13), 4026-4034.
  20. Klar, A. S.; Güven, S.; Biedermann, T.; Luginbühl, J.; Böttcher-Haberzeth, S.; Meuli-Simmen, C.; Meuli, M.; Martin, I.; Scherberich, A.; Reichmann, E., Tissue-engineered dermo-epidermal skin grafts prevascularized with adipose-derived cells. *Biomaterials* **2014**, *35* (19), 5065-5078.
  21. Vasiliadis, A. V.; Katakalos, K., The Role of Scaffolds in Tendon Tissue Engineering. *Journal of Functional Biomaterials* **2020**, *11* (4), 78.
  22. Lewis, D. M.; Tang, V.; Jain, N.; Isser, A.; Xia, Z.; Gerecht, S. J. A. B. S.; Engineering, Collagen fiber architecture regulates hypoxic sarcoma cell migration. **2018**, *4* (2), 400-409.
  23. Pruitt, H. C.; Lewis, D.; Ciccaglione, M.; Connor, S.; Smith, Q.; Hickey, J. W.; Schneck, J. P.; Gerecht, S. J. M. B., Collagen fiber structure guides 3D motility of cytotoxic T lymphocytes. **2020**, *85*, 147-159.
  24. Riching, K. M.; Cox, B. L.; Salick, M. R.; Pehlke, C.; Riching, A. S.; Ponik, S. M.; Bass, B. R.; Crone, W. C.; Jiang, Y.; Weaver, A. M. J. B. j., 3D collagen alignment limits protrusions to enhance breast cancer cell persistence. **2014**, *107* (11), 2546-2558.
  25. Joyce, E. M.; Liao, J.; Schoen, F. J.; Mayer Jr, J. E.; Sacks, M. S. J. T. A. o. t. s., Functional collagen fiber architecture of the pulmonary heart valve cusp. **2009**, *87* (4), 1240-1249.
  26. Jan, N.-J.; Lathrop, K.; Sigal, I. A. J. I. o.; science, v., Collagen architecture of the posterior pole: high-resolution wide field of view visualization and analysis using polarized light microscopy. **2017**, *58* (2), 735-744.
  27. Yang, Y.-l.; Motte, S.; Kaufman, L. J., Pore size variable type I collagen gels and their interaction with glioma cells. *Biomaterials* **2010**, *31* (21), 5678-5688.
  28. Allen, P.; Melero-Martin, J.; Bischoff, J., Type I collagen, fibrin and PuraMatrix matrices provide permissive environments for human endothelial and mesenchymal progenitor cells to form neovascular networks. *J Tissue Eng Regen Med* **2011**, *5* (4), e74-e86.
  29. Yang, Y.-L.; Leone, L. M.; Kaufman, L. J., Elastic moduli of collagen gels can be predicted from two-dimensional confocal microscopy. *Biophysical journal* **2009**, *97* (7), 2051-2060.
  30. Ryan, E. A.; Mockros, L. F.; Weisel, J. W.; Lorand, L., Structural Origins of Fibrin Clot Rheology. *Biophysical Journal* **1999**, *77* (5), 2813-2826.

31. Piechocka, I. K.; Bacabac, R. G.; Potters, M.; MacKintosh, F. C.; Koenderink, G. H., Structural Hierarchy Governs Fibrin Gel Mechanics. *Biophysical Journal* **2010**, *98* (10), 2281-2289.
32. Gersh, K. C.; Nagaswami, C.; Weisel, J. W., Fibrin network structure and clot mechanical properties are altered by incorporation of erythrocytes. *Thromb Haemost* **2009**, *102* (6), 1169-1175.
33. Jaspers, M.; Pape, A. C. H.; Voets, I. K.; Rowan, A. E.; Portale, G.; Kouwer, P. H. J., Bundle Formation in Biomimetic Hydrogels. *Biomacromolecules* **2016**, *17* (8), 2642-2649.
34. Sasaki, J.-I.; Matsumoto, T.; Egusa, H.; Nakano, T.; Ishimoto, T.; Sohmura, T.; Yatani, H., In vitro engineering of transitional tissue by patterning and functional control of cells in fibrin gel. *Soft Matter* **2010**, *6* (8), 1662-1667.
35. Winer, J. P.; Oake, S.; Janmey, P. A., Non-linear elasticity of extracellular matrices enables contractile cells to communicate local position and orientation. *PloS one* **2009**, *4* (7), e6382.
36. Kouwer, P. H.; Koepf, M.; Le Sage, V. A.; Jaspers, M.; van Buul, A. M.; Eksteen-Akeroyd, Z. H.; Woltinge, T.; Schwartz, E.; Kitto, H. J.; Hoogenboom, R.; Picken, S. J.; Nolte, R. J.; Mendes, E.; Rowan, A. E., Responsive biomimetic networks from polyisocyanopeptide hydrogels. *Nature* **2013**, *493* (7434), 651-5.
37. Wang, Y.; Xu, Z.; Lovrak, M.; Sage, V. A. A.; Zhang, K.; Guo, X.; Eelkema, R.; Mendes, E.; Esch, J. H., Biomimetic Strain-Stiffening Self-Assembled Hydrogels. *Angewandte Chemie* **2020**, *132* (12), 4860-4864.
38. Fernández-Castaño Romera, M.; Lou, X.; Schill, J.; Ter Huurne, G.; Fransen, P. P. K. H.; Voets, I. K.; Storm, C.; Sijbesma, R. P., Strain-Stiffening in Dynamic Supramolecular Fiber Networks. *Journal of the American Chemical Society* **2018**, *140* (50), 17547-17555.
39. Wade, R. J.; Bassin, E. J.; Rodell, C. B.; Burdick, J. A., Protease-degradable electrospun fibrous hydrogels. *Nature Communications* **2015**, *6*.
40. Rahmati, M.; Mills, D. K.; Urbanska, A. M.; Saeb, M. R.; Venugopal, J. R.; Ramakrishna, S.; Mozafari, M., Electrospinning for tissue engineering applications. *Progress in Materials Science* **2021**, *117*, 100721.
41. Tan, G. Z.; Zhou, Y., Electrospinning of biomimetic fibrous scaffolds for tissue engineering: a review. *International Journal of Polymeric Materials and Polymeric Biomaterials* **2019**, *69*, 1-14.
42. Kishan, A. P.; Cosgriff-Hernandez, E. M. *Recent advancements in electrospinning design for tissue engineering applications: A review*; 15493296; John Wiley and Sons Inc.: 2017; pp 2892-2905.
43. Davidson, M. D.; Ban, E.; Schoonen, A. C. M.; Lee, M. H.; D'Este, M.; Shenoy, V. B.; Burdick, J. A., Mechanochemical Adhesion and Plasticity in Multifiber Hydrogel Networks. *Advanced Materials* **2020**, *32* (8).
44. Prince, E.; Kumacheva, E., Design and applications of man-made biomimetic fibrillar hydrogels. *Nature Reviews Materials* **2019**, *4* (2), 99-115.
45. Nagy-Smith, K.; Beltramo, P. J.; Moore, E.; Tycko, R.; Furst, E. M.; Schneider, J. P., Molecular, Local, and Network-Level Basis for the Enhanced Stiffness of Hydrogel Networks Formed from Coassembled Racemic Peptides: Predictions from Pauling and Corey. *ACS Central Science* **2017**, *3*, 586-597.
46. Curvello, R.; Raghuwanshi, V. S.; Garnier, G., Engineering nanocellulose hydrogels for biomedical applications. *Advances in Colloid and Interface Science* **2019**, *267*, 47-61.
47. Wallace, D. G.; Rosenblatt, J., Collagen gel systems for sustained delivery and tissue engineering. *Advanced Drug Delivery Reviews* **2003**, *55* (12), 1631-1649.
48. Avendano, A.; Chang, J. J.; Cortes-Medina, M. G.; Seibel, A. J.; Admasu, B. R.; Boutelle, C. M.; Bushman, A. R.; Garg, A. A.; DeShetler, C. M.; Cole, S. L.; Song\*, J. W., Integrated Biophysical Characterization of Fibrillar Collagen-Based Hydrogels. *ACS Biomaterials Science & Engineering* **2020**, *6* (3), 1408-1417.
49. Kumbar, S. G.; James, R.; Nukavarapu, S. P.; Laurencin, C. T., Electrospun nanofiber scaffolds: engineering soft tissues. *Biomedical Materials* **2008**, *3* (3).

50. Ventre, M.; Netti, P. A., Controlling Cell Functions and Fate with Surfaces and Hydrogels: The Role of Material Features in Cell Adhesion and Signal Transduction. *Gels* **2016**, *2* (1).
51. Cheng, G.; Castelletto, V.; Jones, R. R.; Connon, C. J.; Hamley, I. W., Hydrogelation of self-assembling RGD-based peptides. *Soft Matter* **2011**, *7* (4), 1326-1333.
52. Boekhoven, J.; Stupp, S. I., 25th anniversary article: supramolecular materials for regenerative medicine. *Adv Mater* **2014**, *26* (11), 1642-1659.
53. Greenfield, M. A.; Hoffman, J. R.; Olvera de la Cruz, M.; Stupp, S. I., Tunable Mechanics of Peptide Nanofiber Gels. *Langmuir* **2010**, *26* (5), 3641-3647.
54. Prince, E.; Chen, Z.; Khuu, N.; Kumacheva, E., Nanofibrillar Hydrogel Recapitulates Changes Occurring in the Fibrotic Extracellular Matrix. *Biomacromolecules* **2021**, *22* (6), 2352-2362.
55. Warren, N. J.; Rosselgong, J.; Madsen, J.; Armes, S. P., Disulfide-Functionalized Diblock Copolymer Worm Gels. *Biomacromolecules* **2015**, *16* (8), 2514-2521.
56. Taufalele, P. V.; VanderBurgh, J. A.; Muñoz, A.; Zanotelli, M. R.; Reinhart-King, C. A., Fiber alignment drives changes in architectural and mechanical features in collagen matrices. *PLoS One* **2019**, *14* (5), e0216537-e0216537.
57. Motte, S.; Kaufman, L. J., Strain stiffening in collagen i networks. *Biopolymers* **2013**, *99* (1), 35-46.
58. Litvinov, R. I.; Weisel, J. W., Fibrin mechanical properties and their structural origins. *Matrix Biology* **2017**, *60-61*, 110-123.
59. Piechocka, I. K.; Jansen, K. A.; Broedersz, C. P.; Kurniawan, N. A.; MacKintosh, F. C.; Koenderink, G. H., Multi-scale strain-stiffening of semiflexible bundle networks. *Soft Matter* **2016**, *12* (7), 2145-2156.
60. Storm, C.; Pastore, J. J.; MacKintosh, F. C.; Lubensky, T. C.; Janmey, P. A., Nonlinear elasticity in biological gels. *Nature* **2005**, *435* (7039), 191-194.
61. Narasimhan, B. N.; Ting, M. S.; Kollmetz, T.; Horrocks, M. S.; Chalard, A. E.; Malmström, J., Mechanical Characterization for Cellular Mechanobiology: Current Trends and Future Prospects. **2020**, *8* (1333).
62. Broedersz, C. P.; MacKintosh, F. C., Molecular motors stiffen non-affine semiflexible polymer networks. *Soft Matter* **2011**, *7* (7), 3186-3191.
63. Cardoso, L.; Fritton, S. P.; Gailani, G.; Benalla, M.; Cowin, S. C., Advances in assessment of bone porosity, permeability and interstitial fluid flow. *J Biomech* **2013**, *46* (2), 253-265.
64. Elbert, D. L., Liquid-liquid two-phase systems for the production of porous hydrogels and hydrogel microspheres for biomedical applications: A tutorial review. *Acta Biomater* **2011**, *7* (1), 31-56.
65. Qin, X. H.; Wang, X. P.; Rottmar, M.; Nelson, B. J.; Maniura-Weber, K., Near-Infrared Light-Sensitive Polyvinyl Alcohol Hydrogel Photoresist for Spatiotemporal Control of Cell-Instructive 3D Microenvironments. *Advanced Materials* **2018**, *30* (10).
66. Offeddu, G.; Axpe, E.; Harley, B.; Oyen, M., Relationship between permeability and diffusivity in polyethylene glycol hydrogels. *AIP advances* **2018**, *8* (10), 105006.
67. Moreno-Arotzena, O.; Meier, J. G.; Del Amo, C.; García-Aznar, J. M., Characterization of fibrin and collagen gels for engineering wound healing models. *Materials* **2015**, *8* (4), 1636-1651.
68. Zhao, F.; Xiong, Y.; Ito, K.; van Rietbergen, B.; Hofmann, S., Porous Geometry Guided Micro-mechanical Environment Within Scaffolds for Cell Mechanobiology Study in Bone Tissue Engineering. *Frontiers in bioengineering and biotechnology* **2021**, *9*, 736489-736489.
69. Huebsch, N.; Lippens, E.; Lee, K.; Mehta, M.; Koshy, S. T.; Darnell, M. C.; Desai, R. M.; Madl, C. M.; Xu, M.; Zhao, X. H.; Chaudhuri, O.; Verbeke, C.; Kim, W. S.; Alim, K.; Mammoto, A.; Ingber, D. E.; Duda, G. N.; Mooney, D. J., Matrix elasticity of void-forming hydrogels controls transplanted-stem-cell-mediated bone formation. *Nature Materials* **2015**, *14* (12), 1269-1277.
70. Griffin, D. R.; Weaver, W. M.; Scumpia, P. O.; Di Carlo, D.; Segura, T., Accelerated wound healing by injectable microporous gel scaffolds assembled from annealed building blocks. *Nat Mater* **2015**, *14* (7), 737-44.

71. Broguiere, N.; Husch, A.; Palazzolo, G.; Bradke, F.; Madduri, S.; Zenobi-Wong, M., Macroporous hydrogels derived from aqueous dynamic phase separation. *Biomaterials* **2019**, *200*, 56-65.
72. Stachowiak, A. N.; Bershteyn, A.; Tzatzalos, E.; Irvine, D. J., Bioactive Hydrogels with an Ordered Cellular Structure Combine Interconnected Macroporosity and Robust Mechanical Properties. *Advanced Materials* **2005**, *17* (4), 399-403.
73. Grenier, J.; Duval, H.; Barou, F.; Lv, P.; David, B.; Letourneur, D., Mechanisms of pore formation in hydrogel scaffolds textured by freeze-drying. *Acta Biomater* **2019**, *94*, 195-203.
74. Sheikhi, A.; de Rutte, J.; Haghniaz, R.; Akouissi, O.; Sohrabi, A.; Di Carlo, D.; Khademhosseini, A., Microfluidic-enabled bottom-up hydrogels from annealable naturally-derived protein microbeads. *Biomaterials* **2019**, *192*, 560-568.
75. Nih, L. R.; Sideris, E.; Carmichael, S. T.; Segura, T., Injection of Microporous Annealing Particle (MAP) Hydrogels in the Stroke Cavity Reduces Gliosis and Inflammation and Promotes NPC Migration to the Lesion. *Adv Mater* **2017**, *29* (32).
76. Gehlen, D. B.; Jurgens, N.; Omidinia-Anarkoli, A.; Haraszti, T.; George, J.; Walther, A.; Ye, H.; De Laporte, L., Granular Cellulose Nanofibril Hydrogel Scaffolds for 3D Cell Cultivation. *Macromol Rapid Commun* **2020**, *41* (18), e2000191.
77. Seymour, A. J.; Shin, S.; Heilshorn, S. C., 3D Printing of Microgel Scaffolds with Tunable Void Fraction to Promote Cell Infiltration. *Adv Healthc Mater* **2021**, e2100644.
78. Sideris, E.; Griffin, D. R.; Ding, Y.; Li, S.; Weaver, W. M.; Di Carlo, D.; Hsiai, T.; Segura, T., Particle Hydrogels Based on Hyaluronic Acid Building Blocks. *ACS Biomaterials Science & Engineering* **2016**, *2* (11), 2034-2041.
79. Onoe, H.; Okitsu, T.; Itou, A.; Kato-Negishi, M.; Gojo, R.; Kiriya, D.; Sato, K.; Miura, S.; Iwanaga, S.; Kuribayashi-Shigetomi, K.; Matsunaga, Y. T.; Shimoyama, Y.; Takeuchi, S., Metre-long cell-laden microfibres exhibit tissue morphologies and functions. *Nat Mater* **2013**, *12* (6), 584-90.
80. Guerzoni, L. P. B.; Rose, J. C.; Gehlen, D. B.; Jans, A.; Haraszti, T.; Wessling, M.; Kuehne, A. J. C.; De Laporte, L., Cell Encapsulation in Soft, Anisometric Poly(ethylene) Glycol Microgels Using a Novel Radical-Free Microfluidic System. *Small* **2019**, *15* (20), e1900692.
81. Li, W.; Zhang, L.; Ge, X.; Xu, B.; Zhang, W.; Qu, L.; Choi, C. H.; Xu, J.; Zhang, A.; Lee, H.; Weitz, D. A., Microfluidic fabrication of microparticles for biomedical applications. *Chem Soc Rev* **2018**, *47* (15), 5646-5683.
82. Müller, M. Z.; Style, R. W.; Müller, R.; Qin, X.-H., A Phase-separating Thiol-ene Photoresin for Volumetric Bioprinting of Macroporous Hydrogels. *bioRxiv* **2022**, 2022.01.29.478338.
83. Qin, X.-H.; Ovsianikov, A.; Stampfl, J.; Liska, R., Additive manufacturing of photosensitive hydrogels for tissue engineering applications. *BioNanoMaterials* **2014**, *15* (3-4), 49-70.
84. Grigoryan, B.; Paulsen, S. J.; Corbett, D. C.; Sazer, D. W.; Fortin, C. L.; Zaita, A. J.; Greenfield, P. T.; Calafat, N. J.; Gounley, J. P.; Ta, A. H.; Johansson, F.; Randles, A.; Rosenkrantz, J. E.; Louis-Rosenberg, J. D.; Galie, P. A.; Stevens, K. R.; Miller, J. S., BIOMEDICINE Multivascular networks and functional intravascular topologies within biocompatible hydrogels. *Science* **2019**, *364* (6439), 458-+.
85. Zhang, R.; Larsen, N. B., Stereolithographic hydrogel printing of 3D culture chips with biofunctionalized complex 3D perfusion networks. *Lab on a Chip* **2017**, *17* (24), 4273-4282.
86. Qin, X. H.; Wang, X.; Rottmar, M.; Nelson, B. J.; Maniura-Weber, K., Near-Infrared Light-Sensitive Polyvinyl Alcohol Hydrogel Photoresist for Spatiotemporal Control of Cell-Instructive 3D Microenvironments. *Adv Mater* **2018**, *30* (10).
87. Li, Z. Q.; Torgersen, J.; Ajami, A.; Muhleder, S.; Qin, X. H.; Husinsky, W.; Holnthoner, W.; Ovsianikov, A.; Stampfl, J.; Liska, R., Initiation efficiency and cytotoxicity of novel water-soluble two-photon photoinitiators for direct 3D microfabrication of hydrogels. *Rsc Adv* **2013**, *3* (36), 15939-15946.

88. Qin, X. H.; Gruber, P.; Markovic, M.; Plochberger, B.; Klotzsch, E.; Stampfl, J.; Ovsianikov, A.; Liska, R., Enzymatic synthesis of hyaluronic acid vinyl esters for two-photon microfabrication of biocompatible and biodegradable hydrogel constructs. *Polym Chem-Uk* **2014**, *5* (22), 6523-6533.
89. Qin, X. H.; Torgersen, J.; Saf, R.; Muhleder, S.; Pucher, N.; Ligon, S. C.; Holthöner, W.; Redl, H.; Ovsianikov, A.; Stampfl, J.; Liska, R., Three-Dimensional Microfabrication of Protein Hydrogels via Two-Photon-Excited Thiol-Vinyl Ester Photopolymerization. *J Polym Sci Pol Chem* **2013**, *51* (22), 4799-4810.
90. Torgersen, J.; Qin, X.-H.; Li, Z.; Ovsianikov, A.; Liska, R.; Stampfl, J., Hydrogels for Two-Photon Polymerization: A Toolbox for Mimicking the Extracellular Matrix. *Advanced Functional Materials* **2013**, *23* (36), 4542-4554.
91. Sarig-Nadir, O.; Livnat, N.; Zajdman, R.; Shoham, S.; Seliktar, D., Laser Photoablation of Guidance Microchannels into Hydrogels Directs Cell Growth in Three Dimensions. *Biophys J* **2009**, *96* (11), 4743-4752.
92. Arakawa, C.; Gunnarsson, C.; Howard, C.; Bernabeu, M.; Phong, K.; Yang, E.; DeForest, C. A.; Smith, J. D.; Zheng, Y., Biophysical and biomolecular interactions of malaria-infected erythrocytes in engineered human capillaries. *Science Advances* **2020**, *6* (3), eaay7243.
93. Ning, L.; Chen, X., A brief review of extrusion-based tissue scaffold bio-printing. *Biotechnol J* **2017**, *12* (8).
94. Gehlen, J.; Qiu, W.; Schadli, G. N.; Müller, R.; Qin, X. H., Tomographic volumetric bioprinting of heterocellular bone-like tissues in seconds. *Acta Biomater* **2022**.
95. Anindita SN, C. R., Zauchner D, Paunović N, Qiu W, Buzhor MG, et al., Heat-Assisted Digital Light Processing of Bioactive Tough PEG Hydrogels with Complex 3D Structure. *ChemRxiv* **2022**.
96. Wadnap, S.; Krishnamoorthy, S.; Zhang, Z. Y.; Xu, C. X., Biofabrication of 3D cell-encapsulated tubular constructs using dynamic optical projection stereolithography. *J Mater Sci-Mater M* **2019**, *30* (3).
97. Torgersen, J.; Qin, X. H.; Li, Z. Q.; Ovsianikov, A.; Liska, R.; Stampfl, J., Hydrogels for Two-Photon Polymerization: A Toolbox for Mimicking the Extracellular Matrix. *Advanced Functional Materials* **2013**, *23* (36), 4542-4554.
98. Brandenburg, N.; Lutolf, M. P., In Situ Patterning of Microfluidic Networks in 3D Cell-Laden Hydrogels. *Adv Mater* **2016**, *28* (34), 7450-6.
99. Heintz, K. A.; Bregenzler, M. E.; Mantle, J. L.; Lee, K. H.; West, J. L.; Slater, J. H., Fabrication of 3D Biomimetic Microfluidic Networks in Hydrogels. *Adv Healthc Mater* **2016**, *5* (17), 2153-60.
100. Hribar, K. C.; Meggs, K.; Liu, J.; Zhu, W.; Qu, X.; Chen, S. C., Three-dimensional direct cell patterning in collagen hydrogels with near-infrared femtosecond laser. *Sci Rep-Uk* **2015**, *5*.
101. Heintz, K. A.; Mayerich, D.; Slater, J. H., Image-guided, Laser-based Fabrication of Vascular-derived Microfluidic Networks. *J Vis Exp* **2017**, (119).
102. Bhatia, S. N.; Ingber, D. E., Microfluidic organs-on-chips. *Nature biotechnology* **2014**, *32* (8), 760-772.
103. Huh, D.; Matthews, B. D.; Mammoto, A.; Montoya-Zavala, M.; Hsin, H. Y.; Ingber, D. E., Reconstituting organ-level lung functions on a chip. *Science* **2010**, *328* (5986), 1662-1668.
104. Agarwal, T.; Narayana, G. H.; Banerjee, I., Keratinocytes are mechanoresponsive to the microflow-induced shear stress. *Cytoskeleton* **2019**, *76* (2), 209-218.
105. van der Meer, A. D.; Poot, A. A.; Feijen, J.; Vermes, I., Analyzing shear stress-induced alignment of actin filaments in endothelial cells with a microfluidic assay. *Biomicrofluidics* **2010**, *4* (1), 011103.
106. Wang, J.; Heo, J.; Hua, S. Z., Spatially resolved shear distribution in microfluidic chip for studying force transduction mechanisms in cells. *Lab on a Chip* **2010**, *10* (2), 235-239.
107. Naskar, S.; Panda, A. K.; Kumaran, V.; Mehta, B.; Basu, B., Controlled shear flow directs osteogenesis on UHMWPE-based hybrid nanobiocomposites in a custom-designed PMMA microfluidic device. *ACS Applied Bio Materials* **2018**, *1* (2), 414-435.

108. Kim, S.; Kim, H. J.; Jeon, N. L., Biological applications of microfluidic gradient devices. *Integrative Biology* **2010**, *2* (11-12), 584-603.
109. Gilchrist, C. L.; Leddy, H. A.; Kaye, L.; Case, N. D.; Rothenberg, K. E.; Little, D.; Liedtke, W.; Hoffman, B. D.; Guilak, F., TRPV4-mediated calcium signaling in mesenchymal stem cells regulates aligned collagen matrix formation and vinculin tension. *Proc Natl Acad Sci U S A* **2019**, *116* (6), 1992-1997.
110. Verhulsel, M.; Vignes, M.; Descroix, S.; Malaquin, L.; Vignjevic, D. M.; Viovy, J.-L., A review of microfabrication and hydrogel engineering for micro-organs on chips. *Biomaterials* **2014**, *35* (6), 1816-1832.
111. Park, D.; Son, K.; Hwang, Y.; Ko, J.; Lee, Y.; Doh, J.; Jeon, N. L., High-Throughput Microfluidic 3D Cytotoxicity Assay for Cancer Immunotherapy (CACI-IMPACT Platform). **2019**, *10* (1133).
112. Del Amo, C.; Borau, C.; Movilla, N.; Asín, J.; García-Aznar, J. M., Quantifying 3D chemotaxis in microfluidic-based chips with step gradients of collagen hydrogel concentrations. *Integrative Biology* **2017**, *9* (4), 339-349.
113. Takehara, H.; Sakaguchi, K.; Sekine, H.; Okano, T.; Shimizu, T., Microfluidic vascular-bed devices for vascularized 3D tissue engineering: tissue engineering on a chip. *Biomedical Microdevices* **2019**, *22* (1), 9.
114. Correa, S. O.; Luo, X.; Raub, C. B. J. J. o. M.; Microengineering, Microfluidic fabrication of stable collagen microgels with aligned microstructure using flow-driven co-deposition and ionic gelation. **2020**, *30* (8), 085002.
115. Nikolaev, M.; Mitrofanova, O.; Broguiere, N.; Geraldo, S.; Dutta, D.; Tabata, Y.; Elci, B.; Brandenburg, N.; Kolotuev, I.; Gjorevski, N.; Clevers, H.; Lutolf, M. P., Homeostatic mini-intestines through scaffold-guided organoid morphogenesis. *Nature* **2020**, *585* (7826), 574-578.
116. Nasello, G.; Alamán-Díez, P.; Schiavi, J.; Pérez, M. Á.; McNamara, L.; García-Aznar, J. M., Primary human osteoblasts cultured in a 3D microenvironment create a unique representative model of their differentiation into osteocytes. *Frontiers in bioengineering and biotechnology* **2020**, *8*, 336.
117. Homan, K. A.; Gupta, N.; Kroll, K. T.; Kolesky, D. B.; Skylar-Scott, M.; Miyoshi, T.; Mau, D.; Valerius, M. T.; Ferrante, T.; Bonventre, J. V.; Lewis, J. A.; Morizane, R., Flow-enhanced vascularization and maturation of kidney organoids in vitro. *Nature Methods* **2019**, *16* (3), 255-262.
118. Huang, G. Y.; Zhou, L. H.; Zhang, Q. C.; Chen, Y. M.; Sun, W.; Xu, F.; Lu, T. J., Microfluidic hydrogels for tissue engineering. *Biofabrication* **2011**, *3* (1), 012001.
119. Terrell, J. A.; Jones, C. G.; Kabandana, G. K. M.; Chen, C., From Cells-on-a-chip to Organs-on-a-chip: Scaffolding Materials for 3D Cell Culture in Microfluidics. *Journal of Materials Chemistry B* **2020**.
120. Brandenburg, N.; Hoehnel, S.; Kuttler, F.; Homicsko, K.; Ceroni, C.; Ringel, T.; Gjorevski, N.; Schwank, G.; Coukos, G.; Turcatti, G.; Lutolf, M. P., High-throughput automated organoid culture via stem-cell aggregation in microcavity arrays. *Nature Biomedical Engineering* **2020**, *4* (9), 863-874.
121. Fernandez-Yague, M. A.; Abbah, S. A.; McNamara, L.; Zeugolis, D. I.; Pandit, A.; Biggs, M. J., Biomimetic approaches in bone tissue engineering: Integrating biological and physicomaterial strategies. *Adv Drug Deliv Rev* **2015**, *84*, 1-29.
122. Zohar, B.; Blinder, Y.; Mooney, D. J.; Levenberg, S., Flow-induced vascular network formation and maturation in three-dimensional engineered tissue. *ACS Biomaterials Science & Engineering* **2017**, *4* (4), 1265-1271.
123. Baker, B. M.; Trappmann, B.; Stapleton, S. C.; Toro, E.; Chen, C. S., Microfluidics embedded within extracellular matrix to define vascular architectures and pattern diffusive gradients. *Lab on a Chip* **2013**, *13* (16), 3246-3252.
124. Agarwal, T.; Narayana, G. H.; Banerjee, I., Keratinocytes are mechanoresponsive to the microflow-induced shear stress. *Cytoskeleton (Hoboken)* **2019**, *76* (2), 209-218.

125. Elashry, M. I.; Gegnaw, S. T.; Klymiuk, M. C.; Wenisch, S.; Arnhold, S., Influence of mechanical fluid shear stress on the osteogenic differentiation protocols for Equine adipose tissue-derived mesenchymal stem cells. *Acta Histochem* **2019**, *121* (3), 344-353.
126. Uhler, C.; Shivashankar, G. V., Regulation of genome organization and gene expression by nuclear mechanotransduction. *Nat Rev Mol Cell Biol* **2017**, *18* (12), 717-727.
127. Mei, X.; Middleton, K.; Shim, D.; Wan, Q.; Xu, L.; Ma, Y. V.; Devadas, D.; Walji, N.; Wang, L.; Young, E. W. K.; You, L., Microfluidic platform for studying osteocyte mechanoregulation of breast cancer bone metastasis. *Integr Biol (Camb)* **2019**, *11* (4), 119-129.
128. Lee, H. J.; Ewere, A.; Diaz, M. F.; Wenzel, P. L., TAZ responds to fluid shear stress to regulate the cell cycle. *Cell Cycle* **2018**, *17* (2), 147-153.
129. Baker, B. M.; Trappmann, B.; Wang, W. Y.; Sakar, M. S.; Kim, I. L.; Shenoy, V. B.; Burdick, J. A.; Chen, C. S., Cell-mediated fibre recruitment drives extracellular matrix mechanosensing in engineered fibrillar microenvironments. *Nature materials* **2015**, *14* (12), 1262-1268.
130. Polacheck, W. J.; German, A. E.; Mammoto, A.; Ingber, D. E.; Kamm, R. D., Mechanotransduction of fluid stresses governs 3D cell migration. *Proc Natl Acad Sci U S A* **2014**, *111* (7), 2447-52.
131. Wu, J.; Chen, Q.; Liu, W.; He, Z.; Lin, J.-M., Recent advances in microfluidic 3D cellular scaffolds for drug assays. *TrAC Trends in Analytical Chemistry* **2017**, *87*, 19-31.
132. Liu, H.; Wang, Y.; Cui, K.; Guo, Y.; Zhang, X.; Qin, J., Advances in Hydrogels in Organoids and Organs-on-a-Chip. *Advanced Materials* **2019**, *31* (50), 1902042.
133. Millet, M.; Ben Messaoud, R.; Luthold, C.; Bordeleau, F., Coupling Microfluidic Platforms, Microfabrication, and Tissue Engineered Scaffolds to Investigate Tumor Cells Mechanobiology. *Micromachines* **2019**, *10* (6), 418.

## TOC

The review provides an overview of state-of-the-art research on architected hydrogels, including their synthesis, characterization, and fabrication. Emerging applications that leverage architected hydrogels with 3D cell culture and microfluidic technologies towards functional tissue engineering are highlighted.

### Architected Hydrogels for Functional Tissue Engineering Applications

*Doris Zauchner, Monica Zippora Müller, Sophie Zengerle, Adam Aleksander Korczak, Muriel Alexandra Holzreuter and Xiao-Hua Qin\**

